Preparation of polyethyleneimine modification of flower molybdenum disulfide composite(PEI/MoS2) adsorbent and studying it enriched and reduction property for hexavalent chromium from wastewater

Miao Shan Tang
Minnan Normal University
Jian hua Chen (jhchen73@126.com)
Minnan Normal University
JingMei Wang
Minnan Normal University
Qiao Jing Lin
Minnan Normal University
Li Jun Fang
Minnan Normal University

Research Article

Keywords: Flower molybdenum disulfide, Polyethyleneimine, Hexavalent chromium, Adsorption

Posted Date: April 5th, 2021

DOI: https://doi.org/10.21203/rs.3.rs-328094/v1

Preparation of polyethyleneimine modification of flower molybdenum disulfide composite(PEI/MoS_2) adsorbent and studying it enriched and reduction property for hexavalent chromium from wastewater

Miao Shan Tang[1], Jian Hua Chen[1, 2*], Jing Mei Wang [1], Qiao Jing Lin [1], Li Jun Fang[1]

1. College of Chemistry, Chemical Engineering and Environment, Minnan Normal University, Zhangzhou 363000, China
2. Fujian Province University Key Laboratory of Modern Analytical Science and Separation Technology, Minnan Normal University, Zhangzhou 363000, China

Abstract

In this study, flower molybdenum disulfide (MoS_2) was surface-modified with polyethyleneimine(PEI) to prepare PEI/MoS_2 composite adsorbents for Cr(VI) enrichment in aqueous solution. The physicochemical properties of PEI/MoS_2 were characterized by SEM, TEM, XRD, FTIR, BET and XPS methods. The influences of PEI loading, solution pH, contact time, adsorption temperature, and initial Cr(VI) ion concentration on the adsorption performance of PEI/MoS_2 for Cr(VI) were investigated. Under the optimal conditions, and the initial Cr(VI) ion concentration is 50 mg L^{-1}, the adsorption capacity of PEI/MoS_2 is 120.7 mg g^{-1}. The adsorption rate is fast, equilibrium time is 6 h. Competitive adsorption studies of the Cr(VI) , Co(II), Zn(II) and Cd(II) quaternion system were also investigated, the results indicated that selectively adsorbed amount of Cr(VI) on PEI/MoS_2 is significantly higher than that of Co(II), Zn(II) and Cd(II) ions. The adsorption process was spontaneous and conformed to Freundlich isotherm and pseudo-second kinetic model. The consecutive adsorption-desorption experiments indicated that the PEI/MoS_2 has excellent reusability.

Key words: Flower molybdenum disulfide, Polyethyleneimine, Hexavalent chromium, Adsorption

1. Introduction

With the acceleration of the modernization process and the development of industrialization,

* Corresponding author: Chen JH, e-mail: jhchen73@126.com; Phone: 86-596-2591445; Fax: 86-596-2520035

overusing of heavy metals has led to serious environmental pollution (Guo and Yang 2016; Huang et al. 2019). Chromium is commonly used in industrial production, and it has produced a large amount of chromium-containing wastewater mainly containing Cr(VI). Cr(VI) has high toxicity, carcinogenicity, mutagenic ability, non-biodegradability and long-lasting harm to the environment, and is extremely harmful to the natural environment and human beings (Helena. 2012). Chromium is mainly present as trivalent chromium (Cr(III)) and hexavalent chromium (Cr(VI)) in the water environment. However, their toxicity varies greatly. Cr(III) is an essential element, but Cr(VI) is one of the 8 most harmful chemicals in human body (Hamilton et al. 2018; Owlad et al. 2009). Scholars have also conducted more and more researches on chromium-containing wastewater treatment methods. The removal methods mainly include chemical precipitation (Jafari et al. 2013), electrochemical (Dharnaik and Ghosh 2014), ion exchange (Li and Hu 2012), membrane separation (Venkateswaran and Palanivelu 2005), biological method (Mamais et al. 2016) and adso (Liang et al. 2019; Zhang et al. 2020; Khandelwal et al. 2019). Adsorption is the main method to remove Cr(VI) pollutants in water. Numerous adsorbents, such as activated carbon (Enniya et al. 2018; Rai et al. 2016), fly ash (Jahangiri et al. 2018), chitosan (Fan et al. 2020), attapulgite rod (Quan et al. 2014), zeolite (Gaffer et al. 2017), and polymer (Krishnani et al. 2013) have been used. However, most of them exhibit drawbacks, such as high-cost or low adsorption efficiency. Hence, a low-cost adsorbent with high removal efficiency is warranted.

Molybdenum disulfide (MoS_2) is a very typical layered mineral, which belongs to a hexagonal or diamond system and is the principal component of molybdenite. The layered structure of the MoS_2 layer has strong covalent bonds, but the layers are connected by a weak Van der Waals force, so the layers are easier to be peeled off (Chhowalla et al. 2013). Due to this unique structure and properties, it can be widely used in various fields, such as lubricant (Muratore and Voevodin 2006; Farsadi et al. 2017), electrode materials (Feng et al. 2009). MoS_2 has the advantages of large specific surface area and high reactivity, it can be used as a catalyst material (Ghanei and Taher 2018). In addition, MoS_2 has abundant exposure S atoms on the surface, and then sulfur has a strong adhesion to metals, making it hopeful for removing heavy metal ions from water environment (Jia et al. 2018; Chao et al. 2014; Huang et al. 2018). However, as an adsorbent, molybdenum disulfide has the problem of insufficient adsorption sites. In order to improve the adsorption capacity of MoS_2, it is usually used to introduce other functional groups (Chen et al. 2016; Yang et al. 2016) or to compound with other

materials (AghagoLi and Shemirani 2017; Lu et al. 2018).

Polyethyleneimine(PEI) is a partially branched polymer containing primary, secondary, and tertiary amines, and it is a typical polyamine (Bao et al. 2020). It has high reactivity and has a large number of functional groups that can be combined with metal ions. PEI has a wide range of applications, but it is very soluble in water and has the disadvantages of separation and recovery difficulties and easy loss (Chen et al. 2014). The solution to this problem is to carry out grafting or cross-linking modification or to load PEI on other materials to form composite materials, therefore it is more suitable for environmental pollution treatment. For example, immobilizing soluble polyethyleneimine(PEI) nanoclusters within a macroporous cation exchange resin D001 to selective Cu(II) removal (Chen et al. 2010); preparing polyethyleneimine functionalized magnetic Fe_3O_4 using one-step solvothermal method to removal of Pb(II) in an aqueous medium (Jiang et al. 2016)[36].

Because PEI is very soluble in water, it can not be reused when it is used to remove metal ions from wastewater. Pure MoS_2 nanomaterials have the defects of insufficient functional sites, their adsorption capacity for heavy metals is limited. Therefore, in this study, using flower molybdenum disulfide as a carrier, PEI/MoS_2 composite adsorbent were prepared by immobilized PEI onto the surface of MoS_2. The important influence factors, such as reaction time, solution pH, initial Cr(VI) concentration and solution temperature on PEI/MoS_2 adsorption performance for Cr(VI) were studied. The adsorption mechanism and reusability of PEI/MoS_2 was also discussed.

2.Experimental

2.1Materials

The polyethyleneimine(MW=1800) was purchased from Macklin. Diphenyl carbamide was obtained from Sinopharm Chemical Reagent Co., Ltd. All other chemicals were of analytical grade from Xilong Chemical Co., Ltd. Deionized water was used throughout the experiment. $K_2Cr_2O_7$ was used to prepare hexavalent chromium-containing solutions.

2.2 Preparation of PEI/MoS_2 composites adsorbent

Certain amount of $Na_2MoO_4 \cdot 2H_2O$, thiourea (NH_2CSNH_2) and deionized water were added to a 250 mL beaker and continuously stirred until a solution is obtained. Then the solution pH was adjusted to 1.5 using 6 mol.L^{-1} of hydrochloric acid. The obtained solution was placed in a 100 mL Teflon-lined stainless steel reaction kettle and reacted at 230 °C in an oil bath for 20 h. The product

was collected by centrifuged at 10,000 rpm, washed several times with ethanol and deionized water, and then dried under vacuum at 60 ºC for 12 h. Therefore, flower molybdenum disulfide MoS_2 was prepared.

Prepare 100 mL PEI solutions with a concentration of 5, 10, 15, 20 and 25 mg mL^{-1}. Certain amount of MoS_2 was dispersed in the above PEI solutions and sonicated for 10 minutes, and then stirred at room temperature for 12 h, separated by suction filtration, washed the excess PEI with deionized water, and finally dried at 60 ºC. MoS_2 with different PEI loading ratios is recorded as PEI/MoS_2-X(X=5, 10, 15, 20, 25).

2.3 Characterization

The morphology of MoS_2 and PEI/MoS_2 composites adsorbent was observed using scanning electron microscope (SEM, Hitachi S-3400N) and transmission electron microscope (TEM, JEM-2100). The physico-chemical property of MoS_2 and MoS_2-PEI-10 was analyzed by Fourier-transformed infrared spectroscopy (FTIR, Necolet360) and X-ray Diffraction (XRD, D8 Advance). X-ray photoelectron spectroscopy (XPS, K-Alpha+) were performed to determine the surface composition of the adsorbents. The specific surface area of PEI/MoS_2 composites adsorbent was studied by the Brunauer-Emmett-Teller (BET) with an N_2-adsorpmeter.

2.4 Adsorption experiments

$K_2Cr_2O_7$ was used to prepare different concentrations of Cr(VI) solution. Then, appropriate Cr(VI) solutions were added to 50 mL polyethylene vials, and kept PEI/MoS_2 composites adsorbent dose of 0.1g L^{-1} and shaken for enough time at 25 ºC in the shaker. Finally, the solutions were centrifuged separation. The supernate were measured by 1,5-diphenylcarbohydrazide spectrophotometric method using UV-vis spectrophotometer (λ_{max}=540 nm) to observe Cr(VI) concentrations. The adsorption amounts of PEI/MoS_2 composites adsorbent were calculated by the following equation.

$$q_e = (C_0-C_e)v/m \quad (1)$$

where C_0 and C_e (mg L^{-1}) are the initial concentrations and equilibrium concentrations of Cr(VI) solution, respectively; V(mL) is the volume of Cr(VI) solutions; and m(mg) is the dry weight of PEI/MoS_2 composites adsorbent.

3. Results and discussion

3.1 Characterization

3.1.1 SEM and TEM study

Fig. 1(a) shows that the size of the flower MoS_2 is about 200 nm. It is composed of many ultrathin nanosheets with a thickness of several nanometers. From **Fig. 1 (a)**, we also can see that the surface of flower MoS_2 is smooth and has a certain degree of curling, which makes it have a larger surface area and more adsorption sites. After loading PEI, as shown in **Fig. 1 (b)**, the PEI/MoS_2-10 surface became rough. It can be clearly seen in **Fig. 1(c)** and **(d)** that the PEI/MoS_2-10 nanosheets become thicker after loading PEI. This indicates that PEI has been successfully loaded onto the MoS_2 surface.

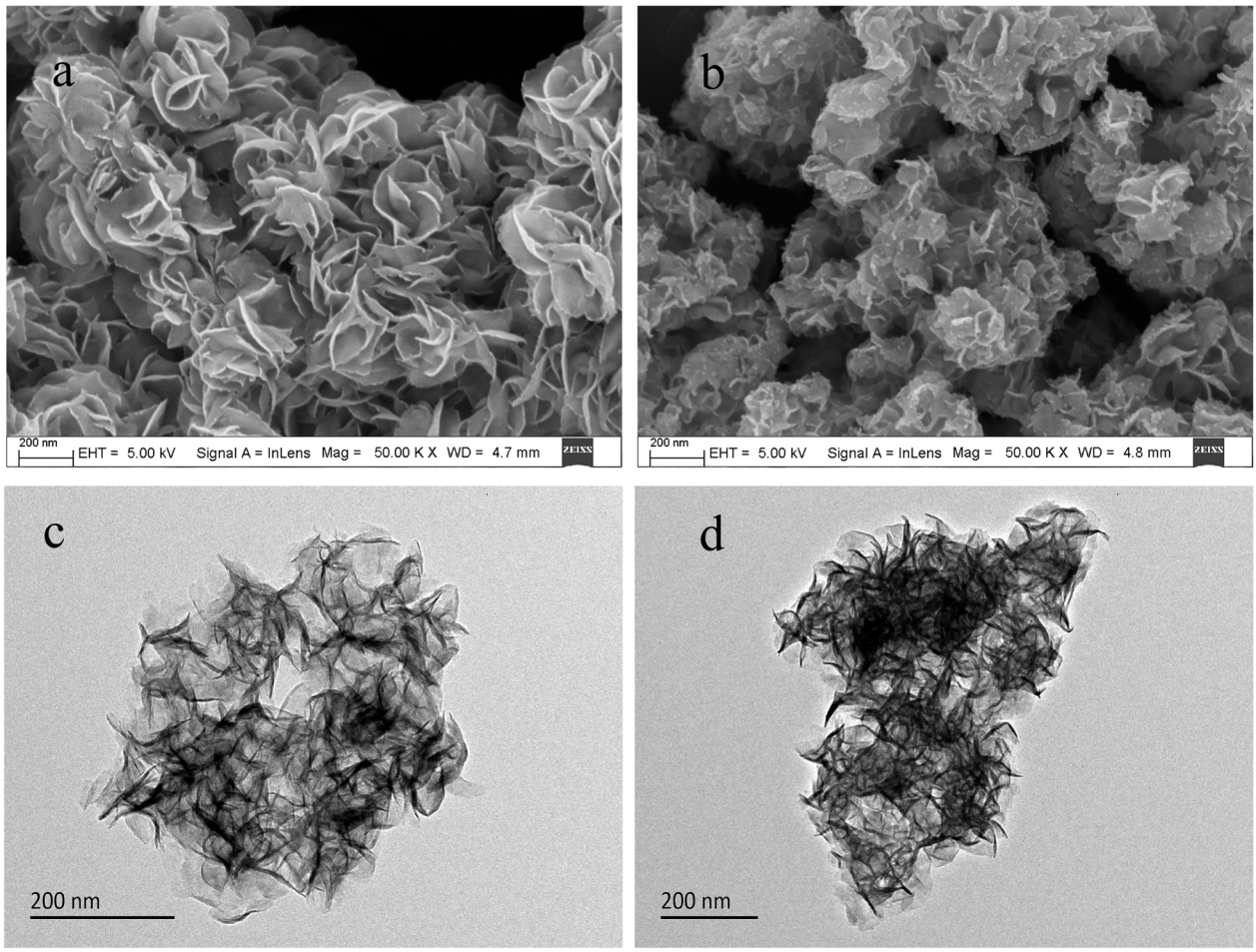

Fig. 1 SEM images of: (a)MoS_2, (b)PEI/MoS_2-10; TEM images of: (c)MoS_2, (d)PEI/MoS_2-10

3.1.2 XRD analysis

XRD images of MoS_2 and PEI/MoS_2-10 composites are exposed in **Fig. 2**. It can be seen that the diffraction peaks of the sample are 13.9°, 32.7°, 39.4° and 58.7°, which correspond to the positions of the characteristic diffraction peaks (002), (100), (103) and (110) in the molybdenum disulfide standard card (PDF#75-1539), respectively. This indicates that MoS_2 was successfully synthesized and highly crystallized. The diffraction peak position and peak intensity of XRD of MoS_2-PEI-10 are consistent with those of MoS_2, which indicates that the loading of PEI will not affect the structure of MoS_2.

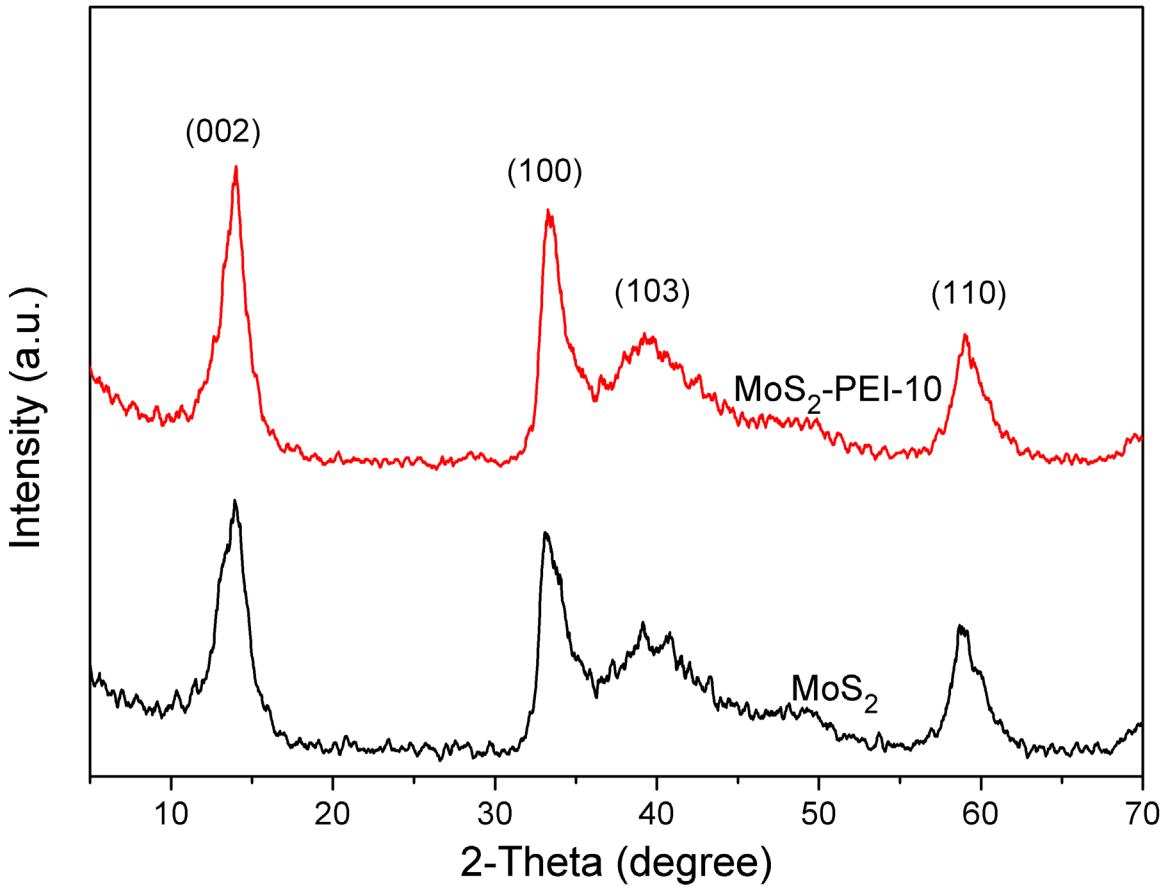

Fig. 2 XRD patterns of MoS_2 and PEI/MoS_2-10 composites

3.1.3 FTIR characterization

Fig. 3 shows the FTIR spectra of MoS_2 and MoS_2-PEI-10. The stretching vibration of Mo-S and stretching vibration of C-N in the thiourea and PEI framework can be seen in the 560 cm^{-1} and 1384 cm^{-1} respectively (Guo et al. 2020). The absorption peaks of amide groups were observed at 1520 and 1634 cm^{-1} (Geng et al. 2019), and the characteristic peaks appearing at 2960 cm^{-1} were related to the methylene of PEI, which proved that PEI has been successfully loaded on the MoS_2. O-H

143 stretching vibration can be seen at 3432 cm^{-1}, which may be physically adsorbed water molecules[38].

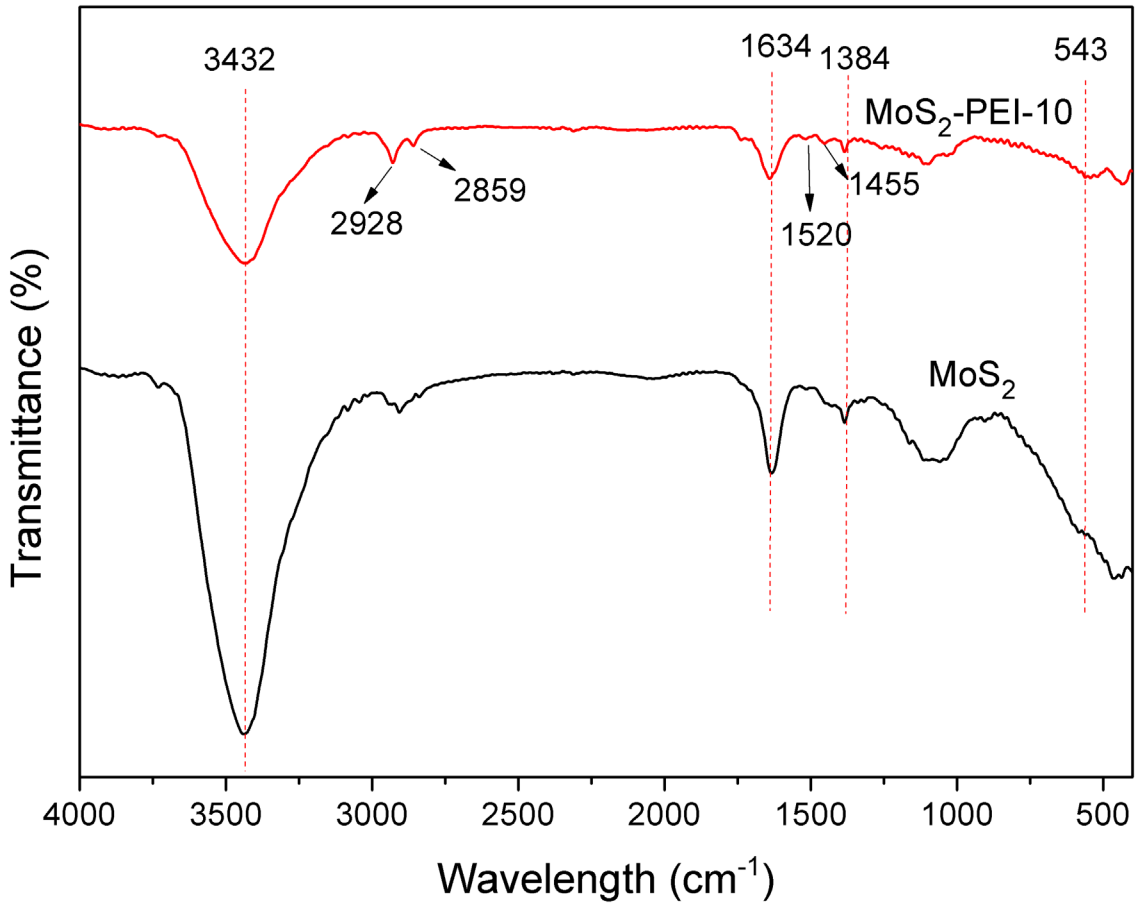

144

145 **Fig. 3** FTIR spectra of MoS_2 and PEI/MoS_2-10

146

147 ### 3.1.4 BET analysis

148 The specific surface area of adsorbent directly affects the contact probability between the
149 adsorbent and the target adsorbate, and the larger the specific surface area, the greater the contact
150 probability. The specific surface area of MoS_2, PEI/MoS_2-10, PEI/MoS_2-15, PEI/MoS_2-20 and
151 PEI/MoS_2-25 were analyzed and shown in **Fig. 4**. The specific surface areas of them are 94.663 m^2
152 g^{-1}, 122.973 m^2 g^{-1}, 45.466 m^2 g^{-1}, 40.234 m^2 g^{-1} and 39.257 m^2 g^{-1}, respectively. The specific surface
153 areas of PEI/MoS_2-10 is largest. This is because the proper loading of PEI increases the specific
154 surface area and provides more adsorption sites. However, excessive loading of PEI on the MoS_2 led
155 to sharp decrease of surface area, which results in the blocking of the lamellar gap of MoS_2 by the
156 PEI.

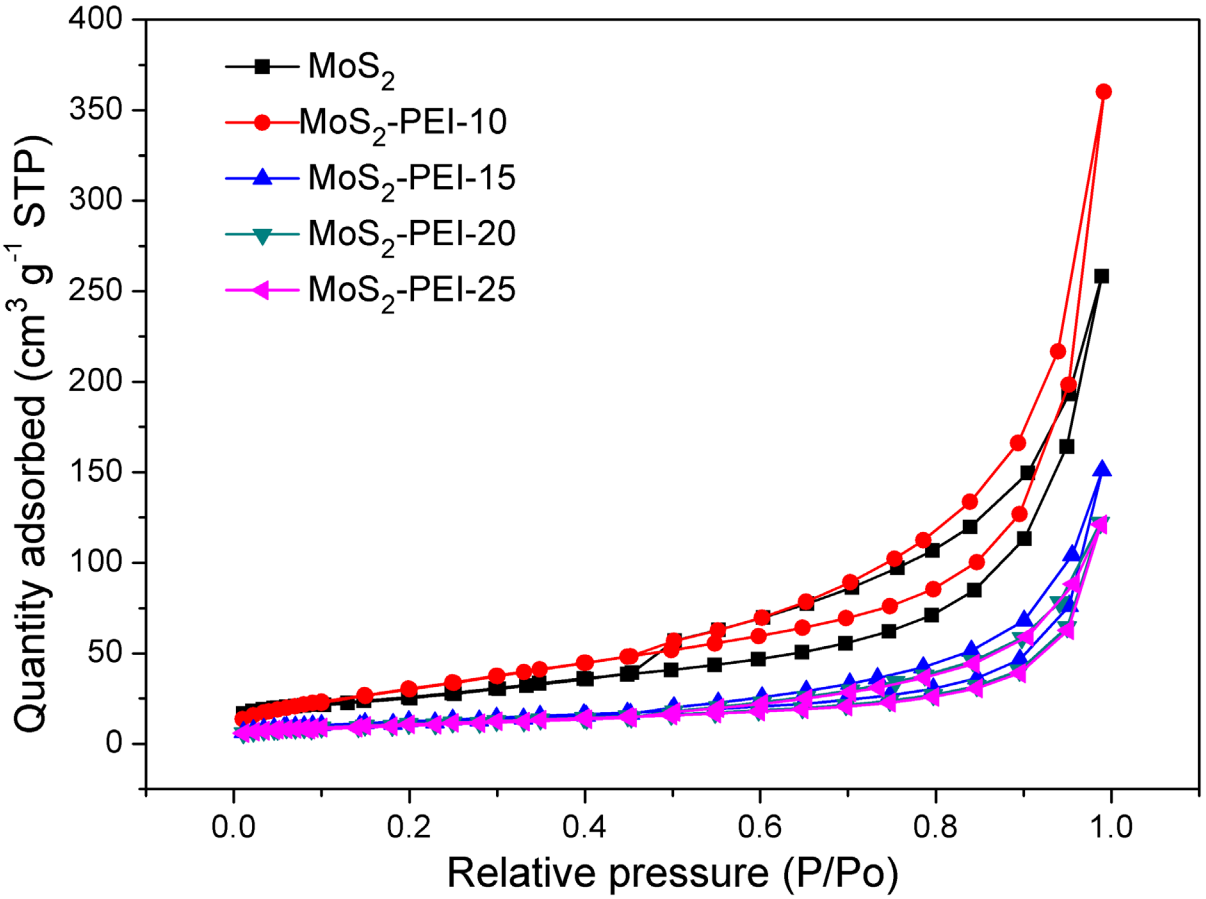

Fig. 4 Nitrogen adsorption-desorption isotherms of MoS_2 and MoS_2-PEI-X

3.2 Effect of PEI loading on Cr(VI) adsorption

In order to study the effect of PEI loading on Cr(VI) adsorption performance of PEI/MoS_2 composites adsorbent, we selected five different PEI loadings of PEI/MoS_2 as adsorbent for Cr(VI) adsorption experiment. As shown in **Fig. 5**, we can see that adsorption capacity of PEI/MoS_2 for Cr(VI) was significantly improved after PEI was loaded on MoS_2. When PEI is loaded on MoS_2, many amino groups (-NH_2) and imino groups (-NH) on PEI are also introduced into PEI/MoS_2, thus enhancing the adsorption capacity of PEI/MoS_2 for Cr (VI) ions. When further increasing of PEI loading from PEI/MoS_2-10 to PEI/MoS_2-25, the adsorption capacity of PEI/MoS_2-X also decreased, which was due to the decrease of the exposed adsorption sites of the PEI/MoS_2-X composite adsorbent due to the excessive PEI loading, which can be proved by BET analysis. In the following experiments, PEI/MoS_2-10 was selected for in subsequent experiments.

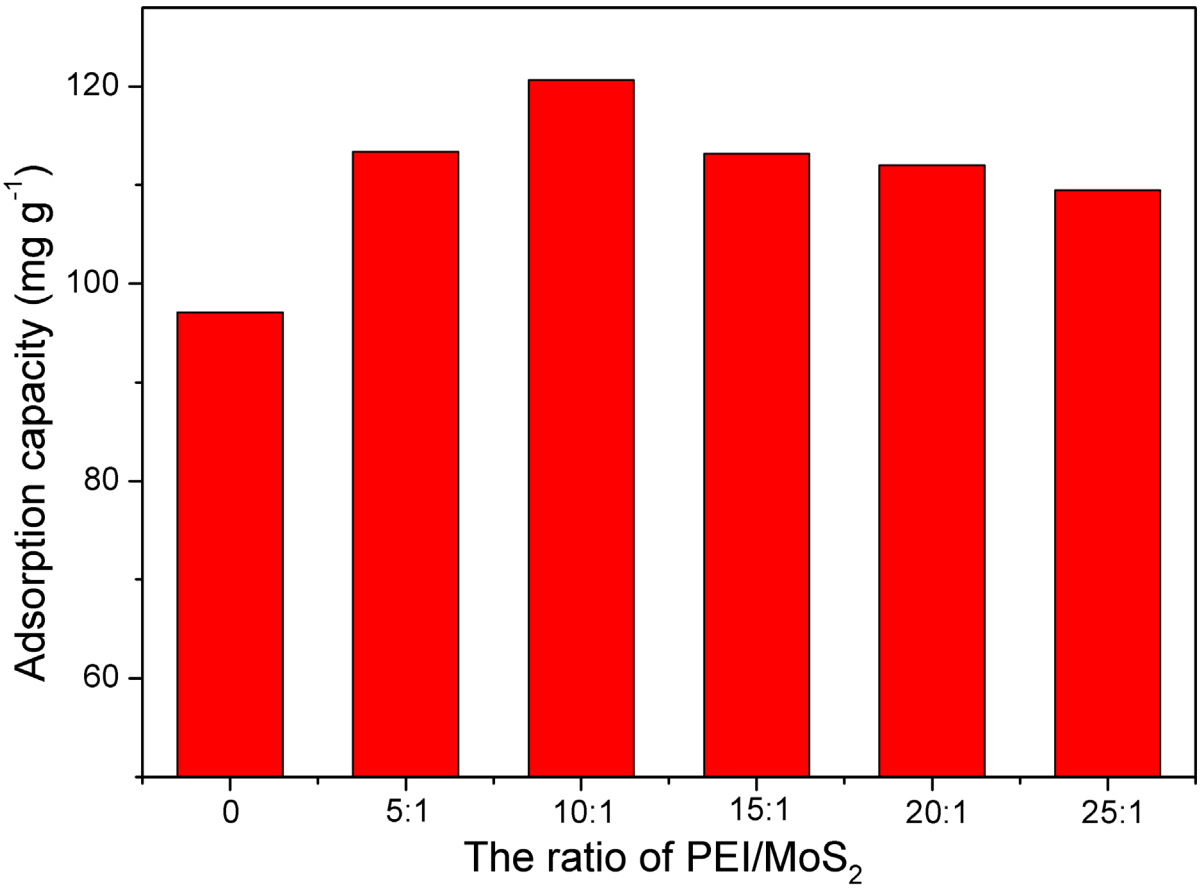

Fig. 5 Effect of PEI loading on PEI/MoS_2-X composites adsorbent on Cr(VI) adsorption

3.3 Adsorption kinetics

Fig. 6 shows the changing of adsorption capacity PEI/MoS_2-10 in Cr(VI) solutions with an initial concentration of 30, 50 and 70 mg L^{-1}. It is shown that the adsorption capacity of PEI/MoS_2-10 for Cr(VI) increased sharply within the first hour, and then increased slowly with the adsorption time. This is can be attributed the amino group (-NH_2) and imino group (=NH) on the surface of the PEI/MoS_2-10 provided a large number of adsorption sites at the beginning of the adsorption, and the concentration of Cr(VI) in the solution was also at the maximum state. At this time, there is a large concentration difference between solvent and the solute, and the adsorption driving force is large. With the increase of the adsorption time, the increase of the adsorption amount is slow because the concentration difference decreases and the driving force weaken. And then the equilibrium state is basically reached after 8 h of adsorption. Therefore, the subsequent experiments used 8 h as the adsorption time for the adsorption equilibrium.

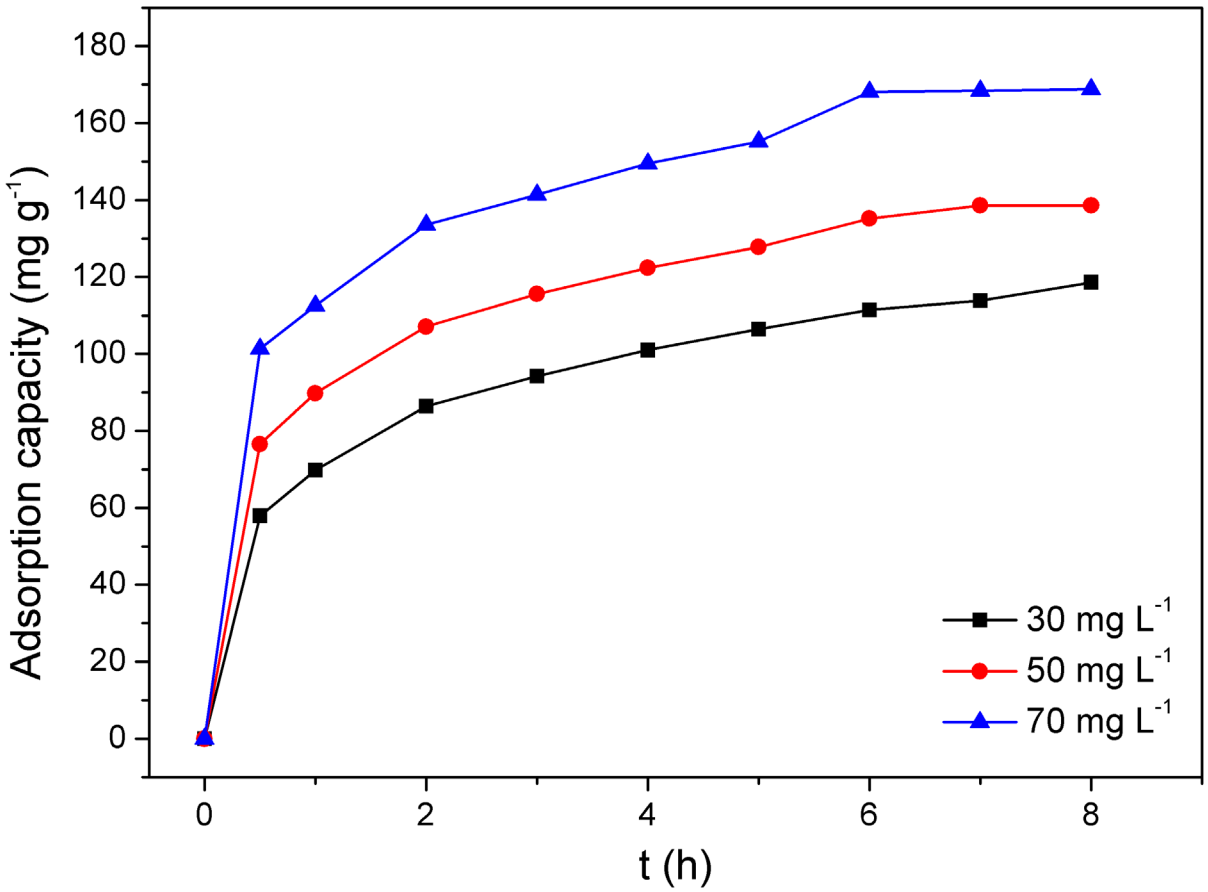

Fig. 6 Effect of adsorption time on Cr(VI) adsorption by PEI/MoS_2-10 at temperature of 25°C

In order to understand better the adsorption behaviors, the quasi-first-order and quasi-second-order kinetic model were used to fit and analyze the adsorption kinetic data.

Quasi-first-order dynamic model equation:

$$q_t = q_e(1-e^{-k_1 t}) \quad (2)$$

Quasi-second-order dynamic model equations:

$$t/q_t = 1/k_2 q_e^2 + t/q_e \quad (3)$$

Where q_e(mg g^{-1}) is the adsorption amount at equilibrium; q_t(mg g^{-1}) is the adsorption amount at time t; k_1(min^{-1}) is the rate constant of the quasi-first-order kinetic model; k_2(g mg^{-1} min^{-1}) is the rate constant of the quasi-second-order kinetic model.

The fitting results are shown in **table 1**. It indicates that the correlation coefficient of quasi-second-order kinetics is significantly higher than that of quasi-first-order kinetics, and the calculated equilibrium adsorption capacity is closer to the actual test results. Therefore, the

quasi-second-order kinetic model is more suitable for describing the process of PEI/MoS_2-10 adsorption of Cr(VI), which indicates that chemical adsorption is a rate-limiting step.

Table 1

Kinetic parameters of Cr (Ⅵ) adsorption by PEI/MoS_2-10

		quasi-first-order kinetic model			quasi-second-order kinetic model		
C_o(mg L^{-1})	q_{exp}(mg g^{-1})	q_{cal}	k_1	R^2	q_{cal}(mg g^{-1})	K_2	R^2
30	118.6	108.3	1.05731	0.9482	122.6	0.01338	0.9884
50	138.6	129.0	1.31280	0.9465	144.7	0.01390	0.9919
70	168.8	156.8	1.52268	0.9373	175.6	0.01259	0.9920

3.4 Effect of pH on Cr(VI) adsorption

The solution pH is one of the important factors affecting the adsorption behavior of the adsorbent, because it affects the existence of metal ions in the aqueous solution as well as the charge density on the surface of the adsorbent. There are five main forms of Cr(VI) in aqueous solution $Cr_2O_7^{2-}$, $HCr_2O_7^-$, CrO_4^{2-}, $HCrO_4^-$ and H_2CrO_4, according the different solution pH. When $2 < pH < 6$, Cr(VI) mainly exists in the form of $HCrO_4^-$ and $Cr_2O_7^{2-}$; $pH > 6$, it mainly exists in the form of CrO_4^{2-}[38]. The effect of solution pH on Cr(VI) adsorption by the PEI/MoS_2-10 composite adsorbent is shown in **Fig. 7**. When the solution pH = 2, the adsorption amount of PEI/MoS_2-10 to Cr(VI) reached the maximum, and the adsorption amount decreased as the pH value increased. This is because the amino group (-NH_2) on the surface of PEI/MoS_2-10 will be protonated (-NH^{3+}) at a low pH value, making the surface of the PEI/MoS_2-10 positively charged, and then the electrostatic force between PEI/MoS_2-10 and negatively charged Cr(VI) is enhanced. As shown in **Fig. 8,** PZC of PEI/MoS_2-10 is 5.6. With the increase of solution pH value(higher than 5.6), the surface group of PEI/MoS_2-10 is deprotonated, resulting in the surface of PEI/MoS_2-10 to be negatively charged and causing electrostatic repulsion with the anion form of Cr(VI). In addition, a large amount of OH^- will competes with the negatively charged Cr(VI) for adsorption sites on the surface of PEI/MoS_2-10 (Saha and Orvig 2010), which greatly reduces the amount of Cr(VI) adsorption.

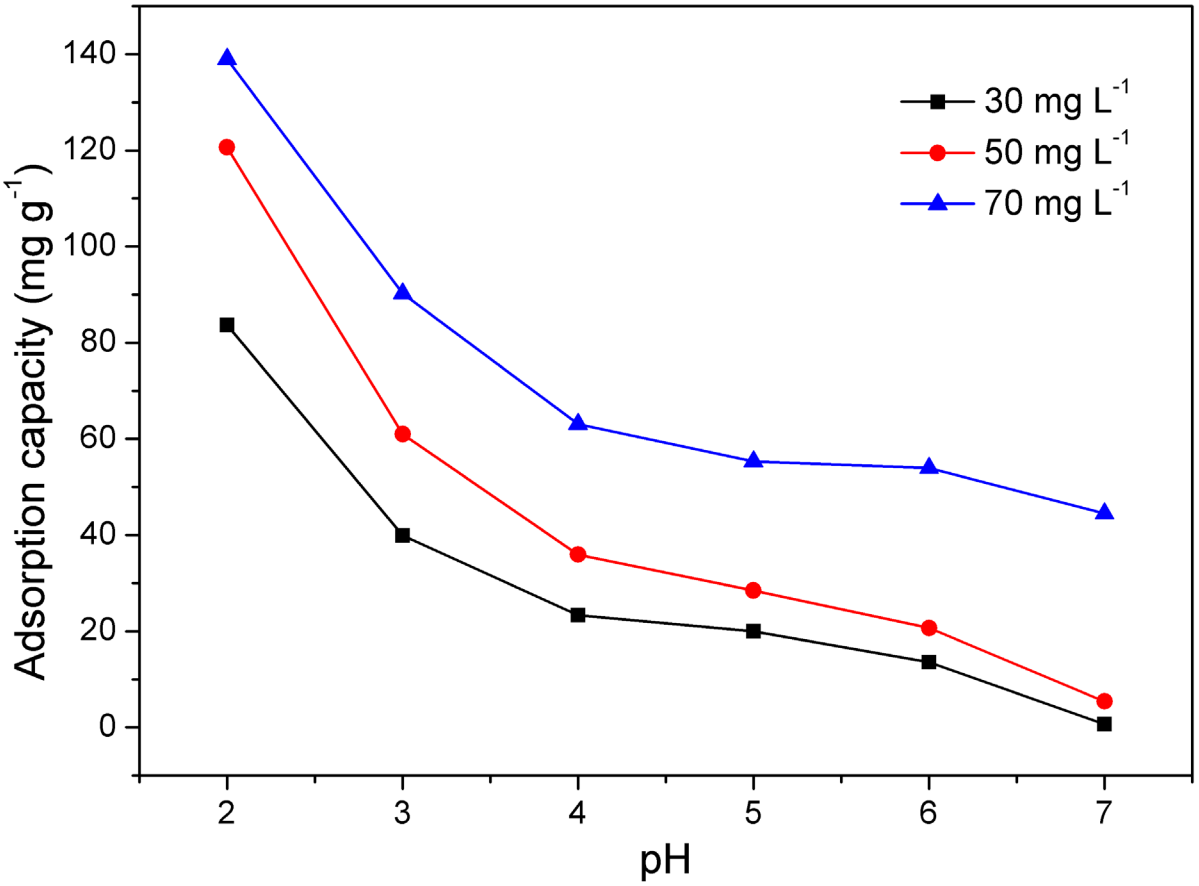

Fig. 7 Effect of solution pH on Cr(VI) adsorption by PEI/MoS_2-10, temperature of 25°C, adsorption time of 6 h

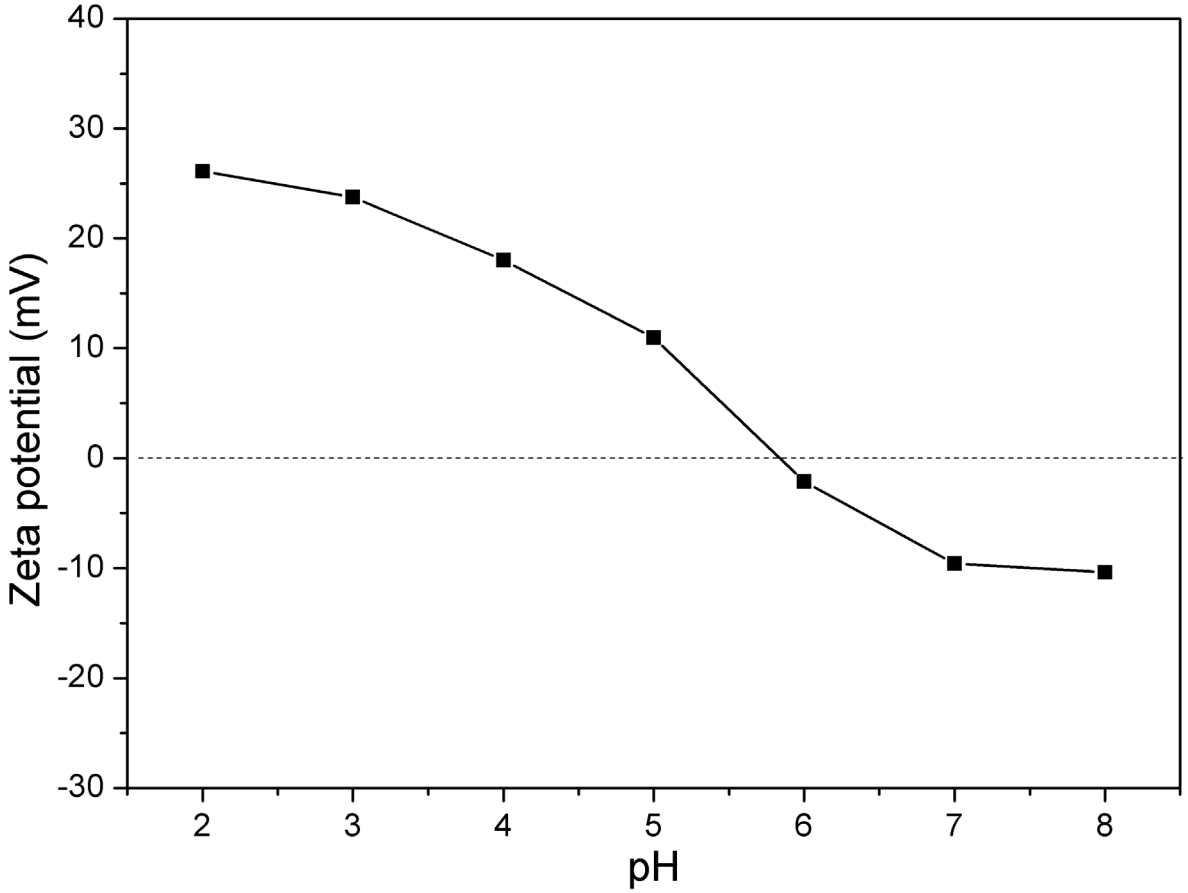

Fig. 8 PZC of PEI/MoS_2-10

3.5 Competitive adsorption

There are many kinds of metal ions in water samples at the same time, so it is very meaningful to study the change of adsorption performance of PEI/MoS_2-10 for Cr(VI) in the presence of multiple ions. In this experiment, Co(II), Zn(II) and Cd(II) were selected as coexist ions to explore the change of adsorption performance of PEI/MoS_2-10 for Cr(VI). **Fig. 9** shows the effect of coexist ions on the adsorption properties of PEI/MoS_2-10. Due to the influence of coexisting ions, the adsorption capacity of PEI/MoS_2-10 for Cr(VI) decreased slightly, which was due to the co-exist ion competition for adsorption sites. However, compared with the other three metal ions, PEI/MoS_2-10 still shows strong selectivity for Cr(VI). This is because PEI/MoS_2-10 has a large number of amino and imino groups. These groups are protonated at low pH value, which makes the surface positively charged and easier to combine with negatively charged Cr(VI) through electrostatic interaction, while Co(II), Zn(II) and Cd(II) in solution coexist in the form of Co^{2+}, Zn^{2+} and Cd^{2+}, it can combine with amino group and imino group through complexation reaction, thus occupying the

adsorption site. However, it has electrostatic repulsion with protonated PEI/MoS_2-10, so the adsorption capacity is low.

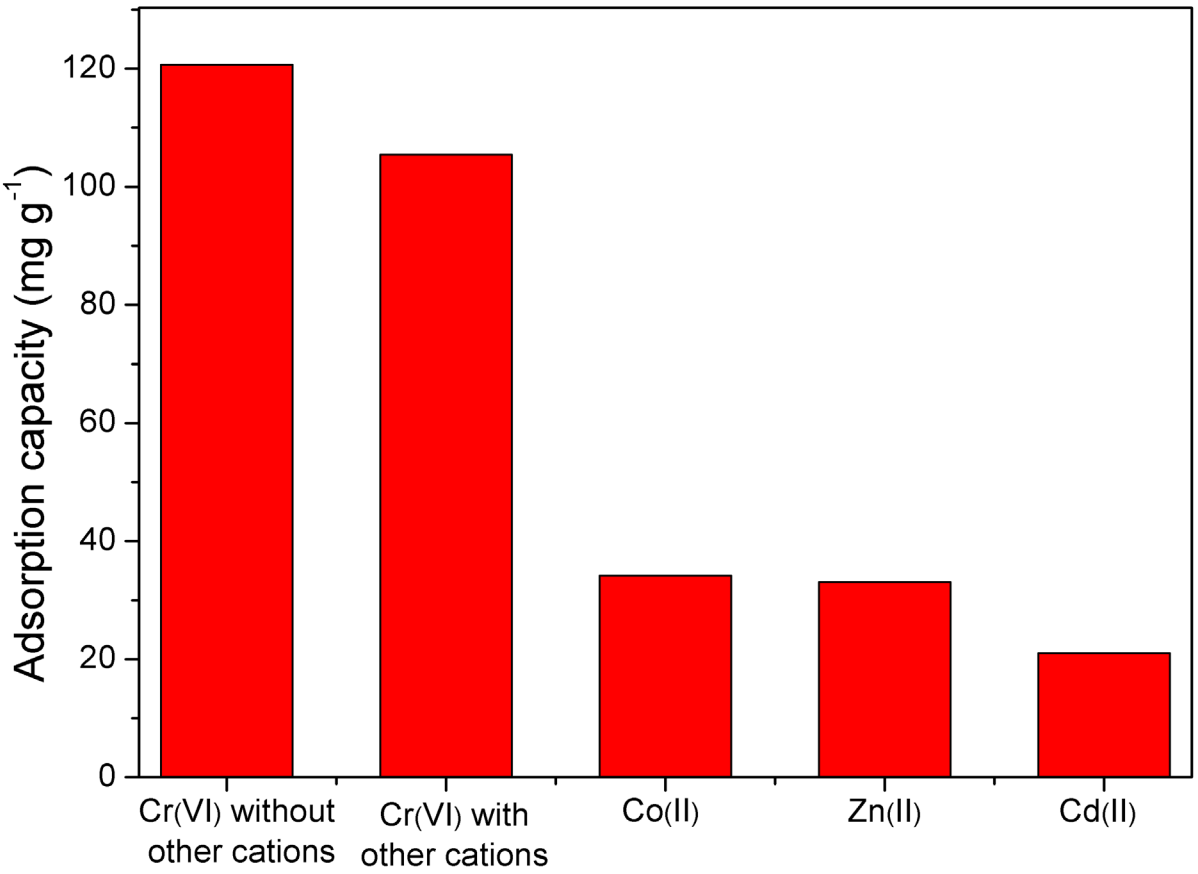

Fig. 9 Effect of interference ion on Cr (VI) adsorption by PEI/MoS_2-10, solution pH of 2, temperature of 25°C, adsorption time of 6 h

3.6 Adsorption isotherms

Fig. 10 shows the effect of initial concentration of Cr(VI) aqueous solution on the adsorption capacity. It shows that the adsorption amount is smaller at a lower Cr(VI) concentration. The possible reason is that the binding site on PEI/MoS_2-10 cannot be fully utilized at a lower ion concentration. When the initial concentration of Cr(VI) solution increases, the adsorption capacity of Cr(VI) increases with the full use of the binding sites on PEI/MoS_2-10.

In this study, Freundlich and Langmuir isotherm model are used to fit the experimental data of Cr(VI) adsorption. The Langmuir isotherm model assumes monolayer adsorption, and the adsorption sites on the adsorbent surface are evenly distributed. The Freundlich isotherm adsorption model describes heterogeneous adsorption, assuming that the molecular layer adsorbs and that the

adsorption sites are unevenly distributed on the surface of the adsorbent.

Freundlich isotherm adsorption model:

$$q_e=k_F c_e^{1/n} \quad (4)$$

$$\ln q_e=(1/n)\ln c_e+\ln k_F \quad (5)$$

Langmuir isotherm adsorption model:

$$q_e=k_L q_{max} c_e/(1+k_l c_e) \quad (6)$$

$$c_e/q_e=c_e/q_{max}+1/(k_l q_{max}) \quad (7)$$

Where c_e and q_e represent the solution concentration (mg L^{-1}) and adsorption amount (mg g^{-1}) at the adsorption equilibrium state; q_{max} represents the adsorption capacity of the adsorbent(mg g^{-1}); k_F(mg g^{-1}.(L $mg^{-1})^{1/n}$) and 1/n represent Freundlich adsorption constants, respectively, represents adsorption capacity and adsorption strength; k_L(L mg^{-1}) represents the Langmuir adsorption constant.

The fit results of the adsorption data for the Freundlich and Langmuir isotherm models are shown in **table 2**. Judging by the values of $\boldsymbol{R^2}$, Freundlich (0.9859) is closer to 1 than Langmuir (0.9456), means that the adsorption of Cr(VI) by PEI/MoS_2-10 is more in line with Freundlich isothermal model. It belongs to multi-layer adsorption, and the adsorption sites are unevenly distributed on the surface of the adsorbent. And 1/n = 0.44 < 1, indicating that the reaction is easy to proceed.

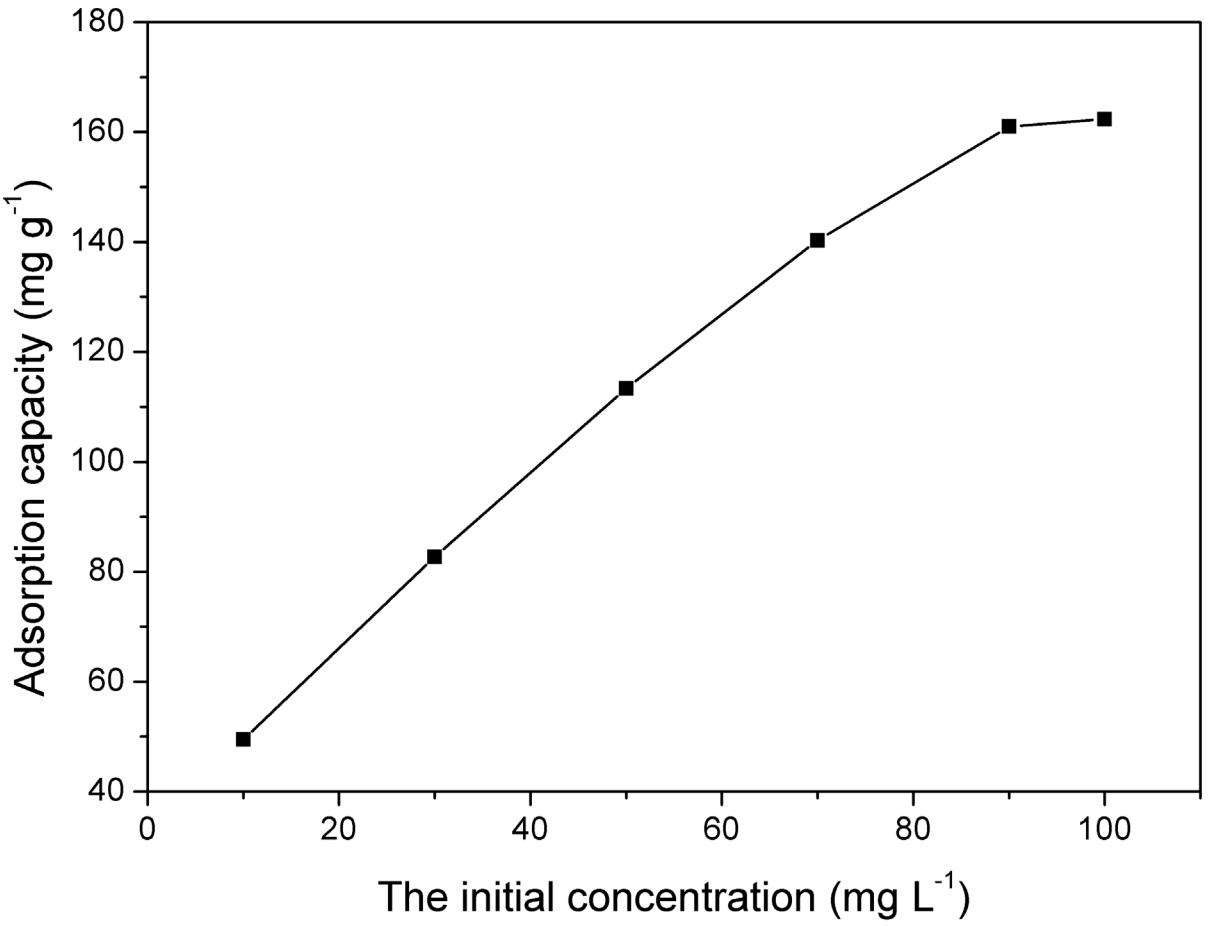

Fig. 10 Effect of initial Cr(VI) concentration on adsorption by PEI/MoS_2-10, solution pH of 2, temperature of 25°C, adsorption time of 6 h

Table 2

Freundlich and Langmuir isotherm parameters

Freundlich			Langmuir		
k_F(mg g^{-1}.(L mg^{-1})$^{1/n}$)	1/n	R^2	q_{max} (mg g^{-1})	k_L(L mg^{-1})	R^2
23.29	0.44	0.9859	208.75	0.038	0.9456

3.7 Adsorption thermodynamics

Fig. 11 shows the PEI/MoS_2-10 adsorption capacity at the temperature of 25, 30, 35, 40 and 45°C. The adsorption of Cr(VI) ions by PEI/MoS_2-10 increased with the increase of temperature, which indicated that the increase of the solution temperature was beneficial to the reaction.

The thermodynamic properties were determined using three thermodynamic data of entropy change (ΔS^0), enthalpy change (ΔH^0) and Gibbs free energy (ΔG^0). The calculation formula is as follows:

$$\ln(q_e/c_e) = -\Delta H / RT + \Delta S / R \quad (8)$$

$$\Delta G = \Delta H - T\Delta S \quad (9)$$

Where ***R***(8.3145 J.mol^{-1}.K^{-1}) represents the ideal gas constant, ***T***(K) represents the absolute temperature. The values of ***ΔH*** and ***ΔS*** can be calculated from the slope and intercept of the straight line obtained by plotting $\ln(q_e/c_e)$ against 1/T.

Table 3 show the calculation results that ***ΔG***<0 show the adsorption process is feasible and spontaneous, and that the ***ΔG*** value decreases as the temperature increases, indicating that the temperature increase is conducive to the progress of the reaction; ***ΔH***>0, indicating that the adsorption process of Cr(VI) by PEI/MoS_2-10 is an endothermic reaction, and the increase in temperature is favorable for the adsorption; ***ΔS***>0, indicating that the disorder increased during the adsorption process.

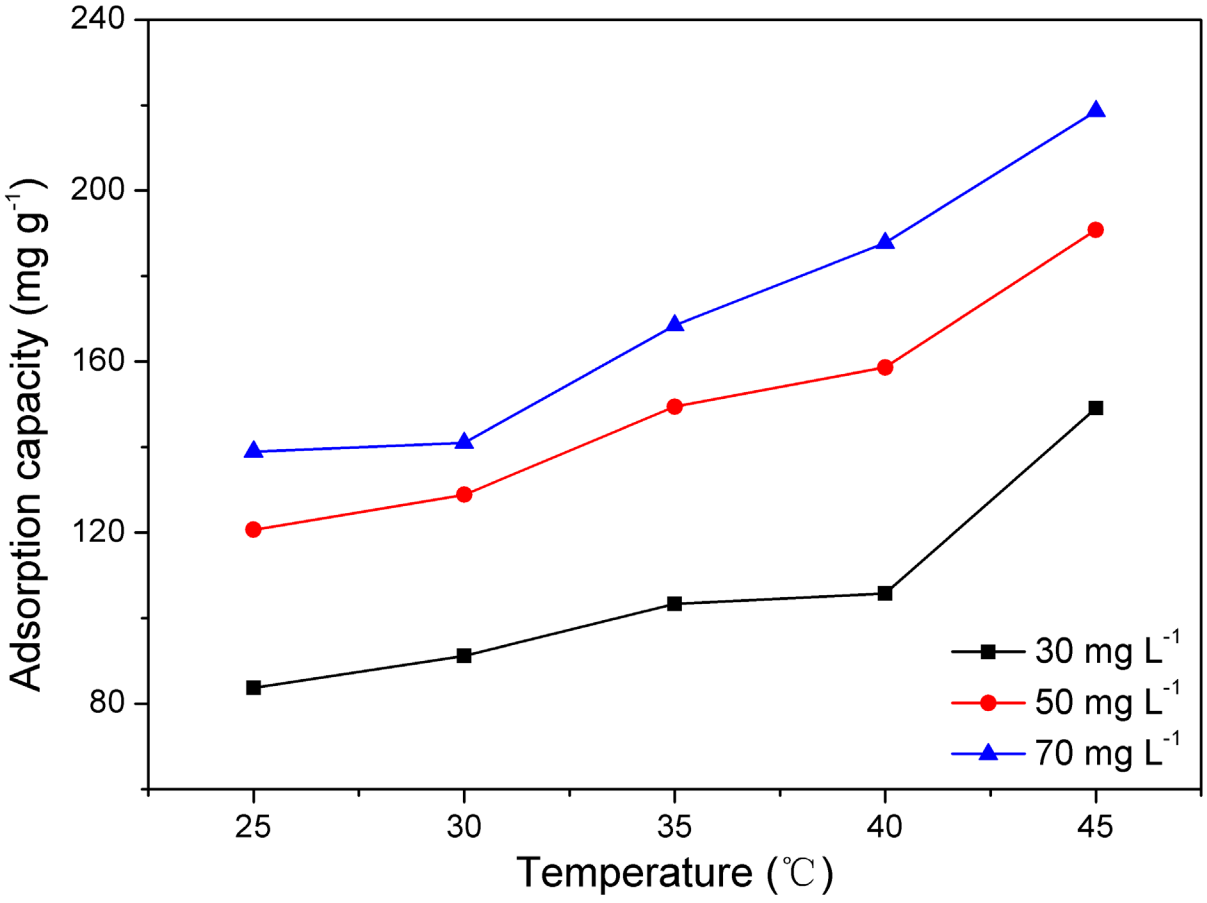

Fig. 11 Effect of temperature on Cr(VI) adsorption, T = 6 h, initial Cr(VI) is 30, 50, 70 mg L^{-1}

Table 3

Thermodynamics parameters

c_o(mg.L^{-1})	Temperature(K)	ΔG^o(kJ.mol^{-1})	ΔH^o(kJ.mol^{-1})	ΔS^o(J.mol^{-1}.k^{-1})
30	298	-3.1487	32.8197	120.70
	303	-3.7521		
	308	-4.3556		
	313	-4.9591		
	318	-5.5626		
50	298	-2.7602	25.4063	94.52
	303	-3.2327		
	308	-3.7053		
	313	-4.1779		
	318	-4.6505		
70	298	-2.0776	24.9092	90.56
	303	-2.5304		
	308	-2.9832		
	313	-3.4360		
	318	-3.8888		

3.8 Reusability Test

The regeneration performance of the PEI/MoS_2-10 composite adsorbent was performed at a solution pH=2 and an initial Cr(VI) concentration o of 50 mg L^{-1}. After adsorption equilibrium, PEI/MoS_2-10 was repeatedly eluted three times with a 0.1 mol L^{-1} NaOH solution, washed several times with deionized water till to neutrality, and then dried for the next adsorption experiment. Repeat the adsorption-desorption four times, and the results are shown in **Fig. 12.** It indicated that PEI/MoS_2-10 own high reusability.

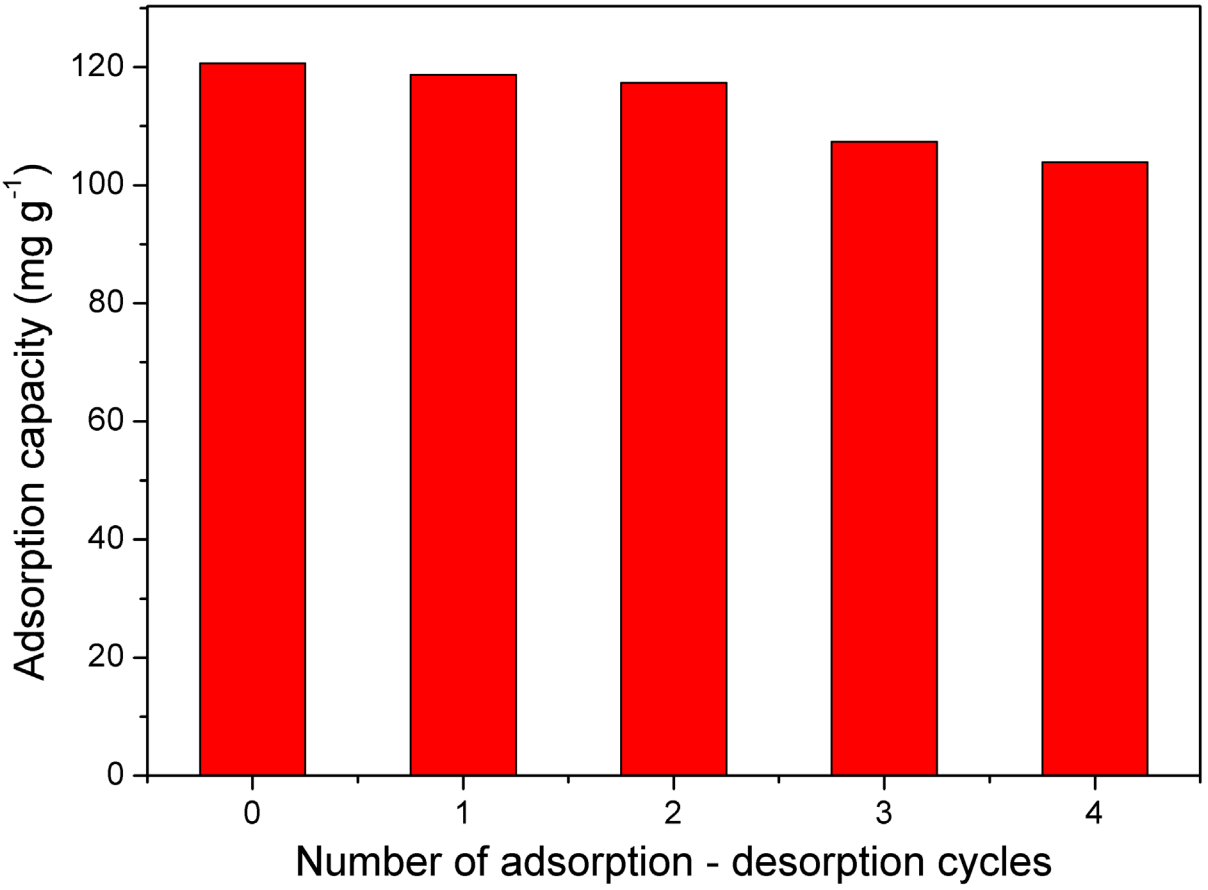

Fig. 12 Cyclic tests of PEI/MoS_2-10, T = 6 h, temperature of 25ºC, initial Cr(VI) is 50 mg L^{-1}

3.9 Adsorption mechanism

Fig. 13 shows the XPS characterization spectrum of Cr 2p after Cr(VI) adsorption by PEI/MoS_2-10. 587.63 eV and 586.57 eV correspond to the Cr 2p1/2 orbit and 578.12 eV and 577.08 eV correspond to the Cr 2p3/2 orbit. The deconvolution of Cr2p XPS peaks was assigned to the peak at 587.63 eV , 578.12 eV for Cr(VI) and 586.57 eV, 577.08 eV for Cr(III). Cr(VI) is adsorbed on the surface of PEI/MoS_2-10 through the hydrogen bonding and electrostatic interaction of amino and imino groups. The existence of Cr(III) indicates that some Cr(VI) ions adsorbed on the surface of PEI/MoS_2-10 were partially reduced to Cr(III) ions. This is because the nitrogen atoms in the amino and imino groups on the surface of the PEI/MoS_2-10 have lone pair electrons and have a certain reducing property, which can reduce the Cr (VI) ions adsorbed on the surface to Cr (III) ions. Therefore, it is speculated that the adsorption process is: (1) the positively charged amino and imino groups adsorb the negatively charged Cr(VI) in the solution to the surface of PEI/MoS_2-10 through electrostatic interaction; (2) the adsorbed Cr(VI)) ions are reduced to Cr(III) ions by amino and

imino groups. Its adsorption process is shown below.

$$-NH_2 + H_3O^+ + HCrO_4^- \rightarrow -NH_3^+ \text{---} HCrO_4^- + H_2O \quad (10)$$

$$=NH + H_3O^+ + HCrO_4^- \rightarrow =NH_2^+ \text{---} HCrO_4^- + H_2O \quad (11)$$

$$HCrO_4^- + 3e^+ + 7\,H^+ \rightarrow Cr^{3+} + 4H_2O \quad (12)$$

$$Cr_2O_7^{2-} + 6e^+ + 7\,H^+ \rightarrow 2Cr^{3+} + 7H_2O \quad (13)$$

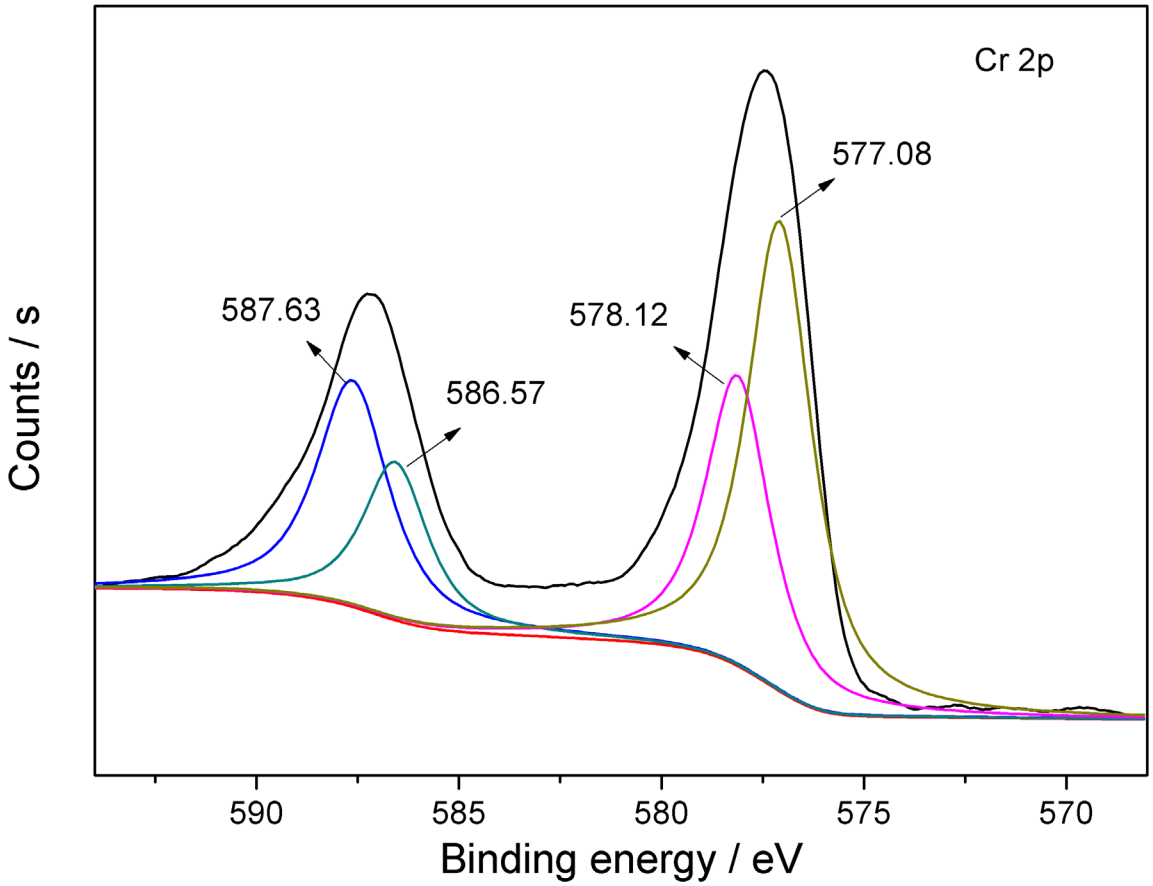

Fig. 13 Binding spectrum of Cr 2p containing chromium

4. Conclusion

In this study, PEI/MoS_2 composites were successfully prepared by modifying the flower MoS_2 with polyethyleneimine (PEI). The experimental results show that PEI/MoS_2-10 has strong Cr(VI) ion enrichment ability. When the solution temperature is 25℃, the solution pH is 2 and the initial Cr(VI) concentration is 50 mg L^{-1}, the adsorption amount of Cr(VI) ions by PEI/MoS_2-10 is 120.7 mg g^{-1} and the equilibrium time is 8 h. Adsorption kinetics can be described by a quasi-second-order kinetic model, and adsorption process conforms to the Freundlich isotherm model. The adsorption process is a spontaneous endothermic process, and the favorable reaction occurs when the

temperature is raised. The successive adsorption-desorption experiments indicated that the MoS_2-PEI-10 is promising for removing and recovering Cr(VI) ions from the aqueous solution.

Ethics approval and consent to participate

Not applicable

Consent for publication

Not applicable

Availability of data and materials

Not applicable

Competing interests

The authors declare that they have no competing interests

Funding

This work is financially supported by the National Natural Science Foundation of China (21676133).

Authors' contributions

The idea for the article (Miaoshan Tang, Jianhua Chen), who performed the literature search and data analysis (Miaoshan Tang, Jingmei Wang, Qiaojing Lin, Lijun Fang), who drafted and/or critically revised the work (Miaoshan Tang, Jianhua Chen), and writing—review and editing (Miaoshan Tang, Jianhua Chen, Jingmei Wang, Qiaojing Lin, Lijun Fang).

Miaoshan Tang, Jianhua Chen, Jingmei Wang, Qiaojing Lin and Lijun Fang read and approved the final manuscript.

Acknowledgements

This work is financially supported by the National Natural Science Foundation of China (21676133).

References

AghagoLi M J, Shemirani F (2017) Hybrid nanosheets composed of molybdenum disulfide and reduced graphene oxide for enhanced solid phase extraction of Pb(II) and Ni(II), Microchim Acta. 184, 237-244.

Bao S T, Yang W W, Wang Y J, Yu Y S, Sun Y Y, Li K F (2020) PEI grafted amino-functionalized graphene oxide nanosheets for ultrafastand high selectivity removal of Cr(VI) from aqueous solutions by adsorptioncombined with reduction: Behaviors and mechanisms, Chem Eng J. 399, 125762.

Chao Y, Zhu W, Wu X, Hou F, Xun S, Wu P, Ji H Y, Xu H, Li H M (2014) Application of graphene-like layered molybdenum disulfide and its excellent adsorption behavior for doxycycline antibiotic, Chem Eng J. 243, 60-67.

Chen B, Zhao X, Liu Y, Xu B, Pan X (2014) Highly stable and covalently functionalized magnetic nanoparticles by polyethyleneimine for Cr(VI) adsorption in aqueous solution. Rsc Adv. 5, 1398-1405.

Chen X, Berner N C, Backes C, Duesberg G S, Mcdonald A R (2016) Functionalization of two-dimensional MoS_2: on the reaction between MoS_2 and organic thiols, Angew Chem Int Ed. 55, 5803-5808.

Chen Y, Pan R, Rnhaiyan L I, Zhang R, Rnlu L V, Rnjun W U (2010) Selective removal of Cu(II) ions by using cation-exchange resin-supported polyethyleneimine (PEI) nanoclusters, Environ ence Technol. 44, 3508-3513.

Chhowalla M, Shin H S, Eda G, Li L J, Loh K P, Zhang H (2013) The chemistry of two-dimensional layered transition metal dichalcogenide nanosheets, Nat Chem. 5, 263-275.

Dharnaik A S, Ghosh P K (2014) Hexavalent chromium [Cr(VI)] removal by the electrochemical ion-exchange process, Environ Technol. 35(18), 2272-2279.

Enniya I, Rghioui L, Jourani A (2018) Adsorption of hexavalent chromium in aqueous solution on activated carbon prepared from apple peels, Sustain. Chem Pharm. 7, 9-16.

Fan H L, Ren H Y, Ma X Z, Zhou S F, Huang J, Jiao W Z, Qi G S, Liu Y Z (2020) High-gravity continuous preparation of chitosan-stabilized nanoscale zerovalent iron towards Cr(VI) removal, Chem Eng J. 390, 124639.

Farsadi M, Bagheri S, Ismail N A (2017) Nanocomposite of functionalized graphene and molybdenum disulfide as friction modifier additive for lubricant, J Mol liq. 244, 304-308.

Feng C, Ma J, Li H, Zeng R, Guo Z, Liu H (2009) Synthesis of molybdenum disulfide (MoS_2) for lithium ion battery applications, Mater Res Bull. 44(9), 1811-1815.

Gaffer A, Kahlawy A A Al, Aman D (2017) Magnetic zeolite-natural polymer composite for

393 adsorption of chromium (VI), Egypt J Pet. 2, 995-999.
394 Geng J J, Yin Y W, Liang Q W, Zhu Z J, Luo H J (2019) Polyethyleneimine cross-linked graphene
395 oxide for removing hazardous hexavalent chromium: Adsorption performance and mechanism,
396 Chem Eng J. 361,1497-1510.
397 Ghanei-Motlagh M, Taher M A (2018) A novel electrochemical sensor based on silver/halloysite
398 nanotube/molybdenum disulfide nanocomposite for efficient nitrite sensing, Biosens Bioelectron.
399 109, 279-285.
400 Guo D X, Song X M, Zhang L L, Chen W W, Chu D W, Tan L C (2020) Recovery of uranium(VI)
401 from aqueous solutions by the polyethyleneimine-functionalized reduced graphene
402 oxide/molybdenum disulfide composition aerogels, J Taiwan Inst Chem E. 106, 198-205.
403 Guo Y, Yang S (2016) Heavy metal enrichments in the Changjiang (Yangtze River) catchment and on
404 the inner shelf of the East China Sea over the last 150 years, Sci Total Environ. 543, 105-115.
405 Hamilton E M, Young S D, Bailey E H, Watts M J (2018) Chromium speciation in foodstuffs: a
406 review, Food Che. 250, 105-112.
407 Helena O (2012) Chromium as an environmental pollutant: insights on induced plant toxicity, J Bot.
408 2012, 1-8.
409 Huang Q, Zhao J, Liu M Y (2018) Synthesis of polyacrylamide immobilized molybdenum disulfide
410 (MoS_2@PDA@PAM) composites via mussel-inspired chemistry and surface-initiated atom transfer
411 radical polymerization for removal of copper (II) ions, J Taiwan Inst Chem E. 86, 174-184.
412 Huang Y Y, Zhou B H, Nan L, Li Y M, Han R R, Qi J C, Lu X H, Li S, Feng C Y, Liang S (2019)
413 Spatial-temporal analysis of selected industrial aquatic heavy metal pollution in china, J Clean Prod.
414 238, 117944.
415 Jafari A J, Golbaz S, Kalantary R R (2013) Treatment of hexavalent chromium by using a combined
416 fenton and chemical precipitation process, J Water Reuse Desalination. 3, 373-380.
417 Jahangiri K, Yousefi N, Ghadiri S K, Fekri R, Bagheri A, Talebi S S (2018) Enhancement adsorption
418 of hexavalent chromium onto modified fly ash from aqueous solution; optimization; isotherm,
419 kinetic and thermodynamic study, J Disper Sci Technol. 2018, 1-12.
420 Jia F, Liu C, Yang B, Zhang X, Yi H, Ni J, Song S (2018) Thermal modification of molybdenum
421 disulfide surface for tremendous improvement of Hg^{2+} adsorption from aqueous solution, ACS
422 Sustain Chem Eng. 6, 9065-9073.

Jiang H, Sun M, Xu J, Lu A, Shi Y (2016) Magnetic Fe_3O_4 nanoparticles modified withpolyethyleneimine for the removal of Pb(II), Clean. 44, 1146-1153.

Khandelwal N, Singh N, Tiwari E, Darbha G K (2019) Novel synthesis of a clay supported amorphous aluminum nanocomposite and its application in removal of hexavalent chromium from aqueous solutions, RSC Adv. 9, 11160-11169.

Krishnani K K, Srinives S, Mohapatra B C, Boddu V M, Hao J, Meng X, Muchandani A (2013) Hexavalent chromium removal mechanism using conducting polymers, J Hazard Mater. 252-253, 99-106.

Li Z Y, Hu S (2012) Removal of Hexavalent Chromium from Aqueous Solutions by Ion-Exchange Resin. Adv Mat Res. 550-553, 2333-2337.

Liang H X, Song B, Peng P, Jiao G J, Yan X, She D (2019) Preparation of three-dimensional honeycomb carbon materials and their adsorption of Cr(VI), Chem Eng J. 367, 9-16.

Lu Y, Fang Y Y, Xiao X D, Qi S, Huan C M, Zhan Y J, Cheng H L, Xu G (2018) Petal-like molybdenum disulfide-loaded nanofibers membrane with superhydrophilic property for dye adsorption, Colloid Surface A. 553, 210-217.

Mamais D, Noutsopoulos C, Kavallari I, Nyktari E, Kaldis A, Panousi E, Nikitopoulos G, Antoniou K, Nasioka M (2016) Biological groundwater treatment for chromium removal at low hexavalent chromium concentrations, Chemosphere. 152, 238-244.

Muratore C, Voevodin A A (2006) Molybdenum disulfide as a lubricant and catalyst in adaptive nanocomposite coatings, Surf Coat Tech. 201, 4125-4130.

Owlad M, Aroua M K, Daud W A W, Baroutian S (2009) Removal of hexavalent chromium-contaminated water and wastewater: a review, Water Air Soil Poll. 200, 59-77.

Quan G, Zhang J, Guo J, Lan Y (2014) Removal of Cr(VI) from Aqueous Solution by Nanoscale Zero-Valent Iron Grafted on Acid-Activated Attapulgite, Water Air Soil Poll. 225, 1979.

Venkateswaran P, Palanivelu K (2005) Studies on recovery of hexavalent chromium from plating wastewater by supported liquid membrane using trinbutyl phosphate as carrier, Hydrometallurgy. 78, 107-115.

Rai M K, Shahi G, Meena V, Meena R, Chakraborty S, Singh R S, Rai B N (2016) Removal of hexavalent chromium Cr(VI) using activated carbon prepared from mango kernel activated with H_3PO_4, Resour Effi Technol. 2, 63-70.

453 Saha B, Orvig C (2010) Biosorbents for hexavalent chromium elimination from industrial and
454 municipal effluents, Coordin Chem Rev. 254, 2959-2972.
455 Yang X, Meng N N, Zhu Y C, Zhou Y F, Nie W Y, Chen P P (2016) Greatly improved mechanical
456 and thermal properties of chitosan by carboxyl-functionalized MoS_2 nanosheets, J Mater Sci. 51,
457 1344-1353.
458 Zhang S J, Shi Q T, Korfiatis G, Christodoulatos C, Wang H J, Meng X G (2020) Chromate removal
459 by electrospun PVA/PEI nanofibers: adsorption, reduction, and effects of co-existing ions, Chem Eng
460 J. 387, 124179.

Figures

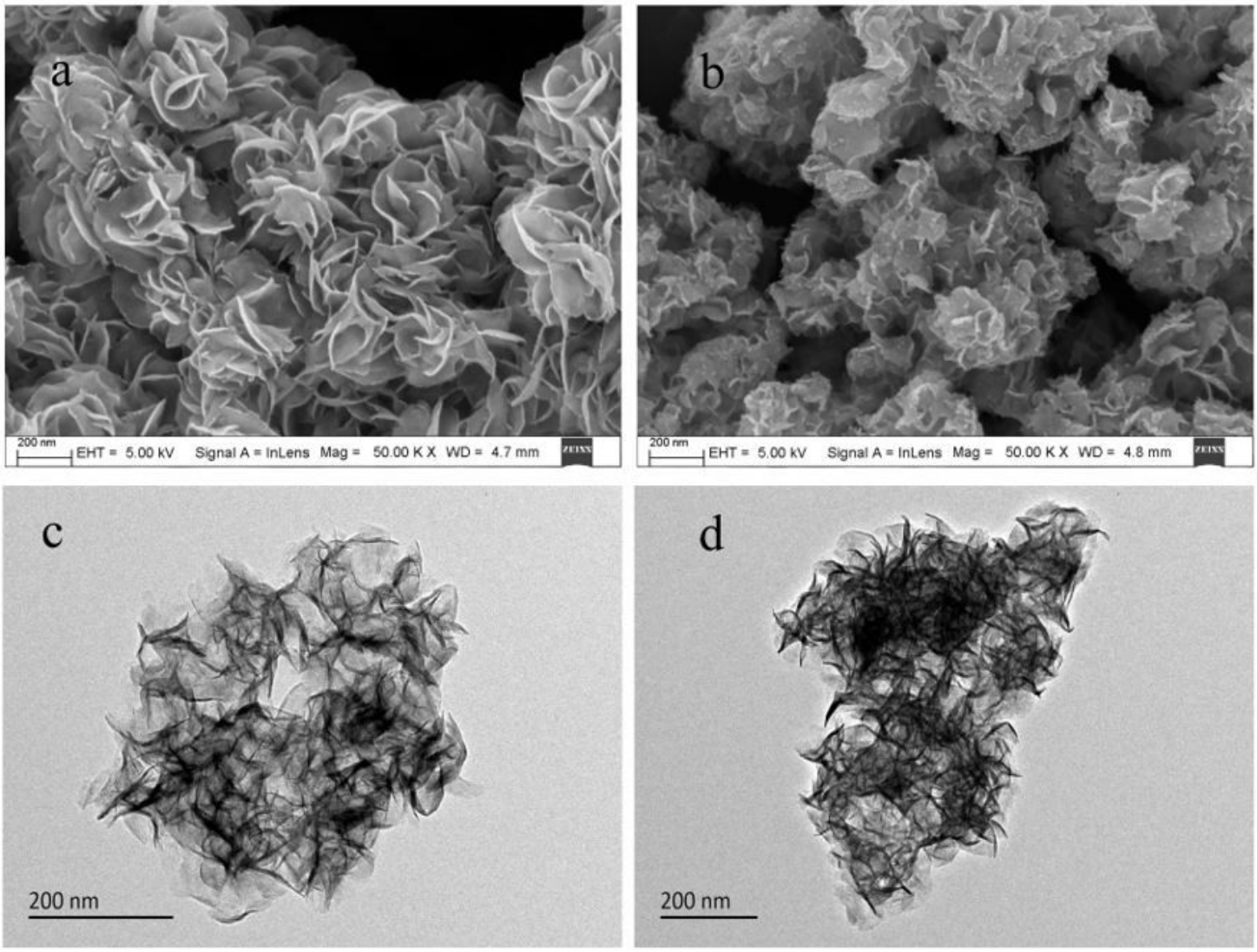

Figure 1

SEM images of: (a)MoS2, (b)PEI/MoS2-10; TEM images of: (c)MoS2, (d)PEI/MoS2-10

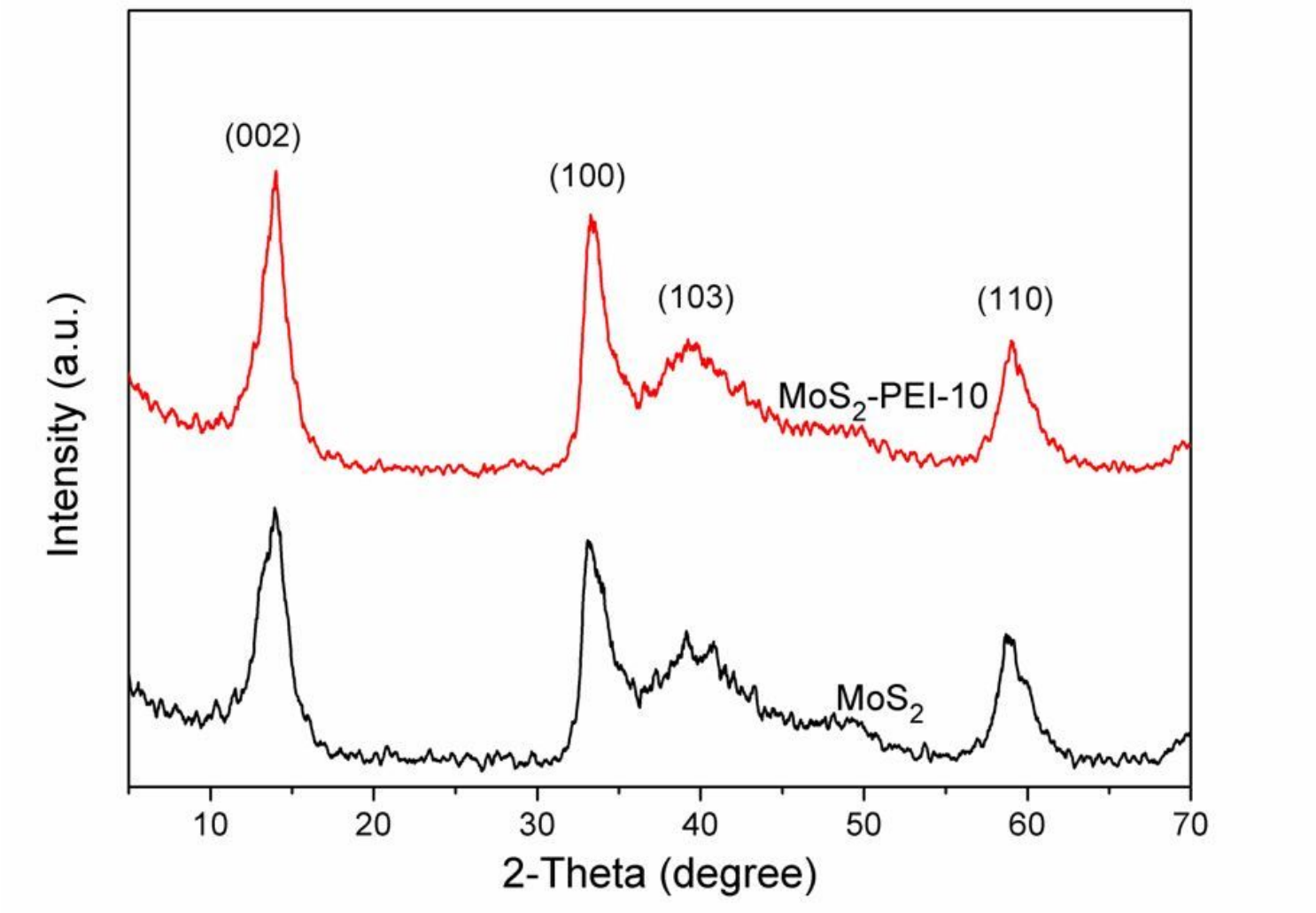

Figure 2

XRD patterns of MoS2 and PEI/MoS2-10 composites

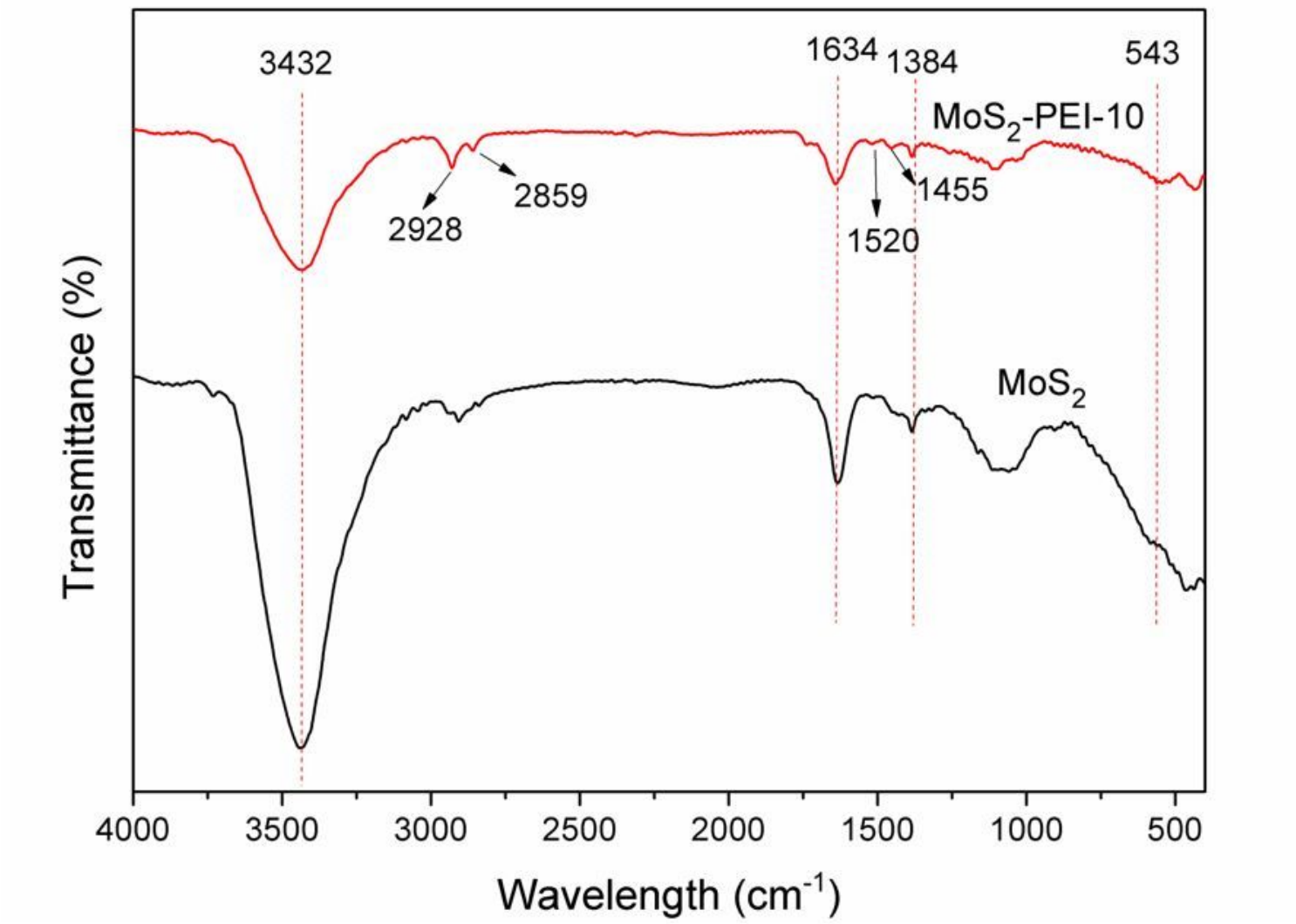

Figure 3

FTIR spectra of MoS2 and PEI/MoS2-10

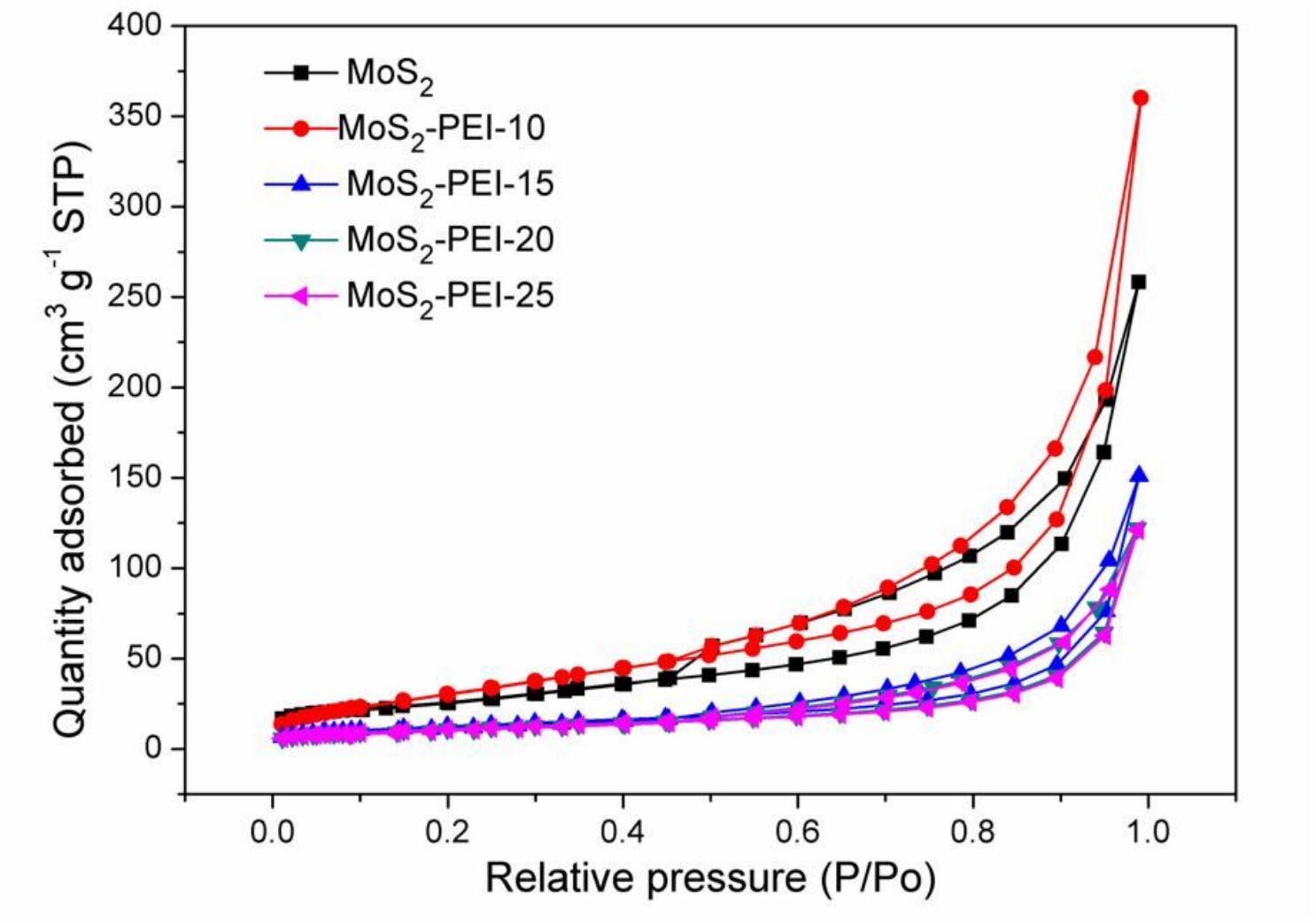

Figure 4

Nitrogen adsorption-desorption isotherms of MoS2 and MoS2-PEI-X

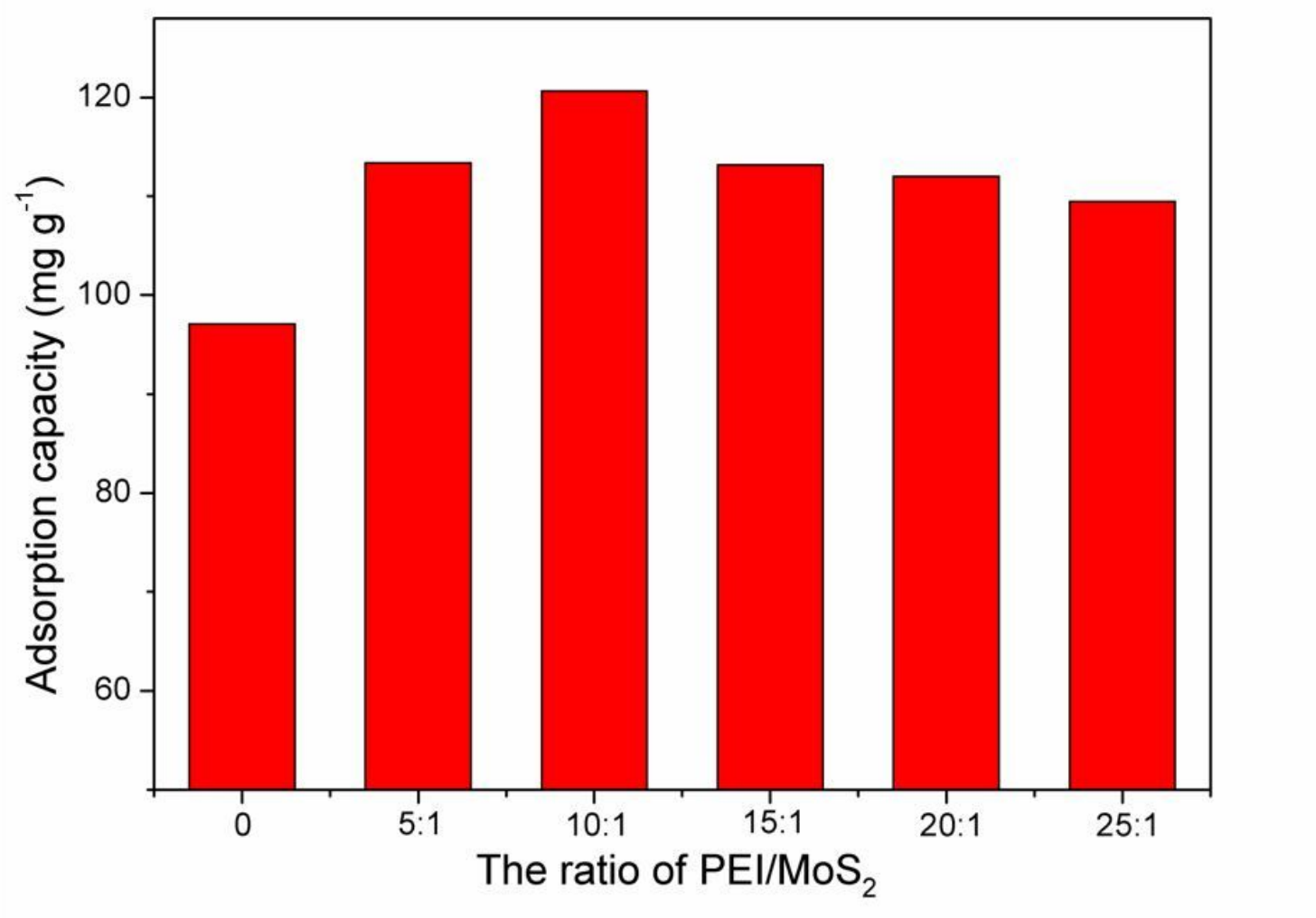

Figure 5

Effect of PEI loading on PEI/MoS2-X composites adsorbent on Cr(VI) adsorption

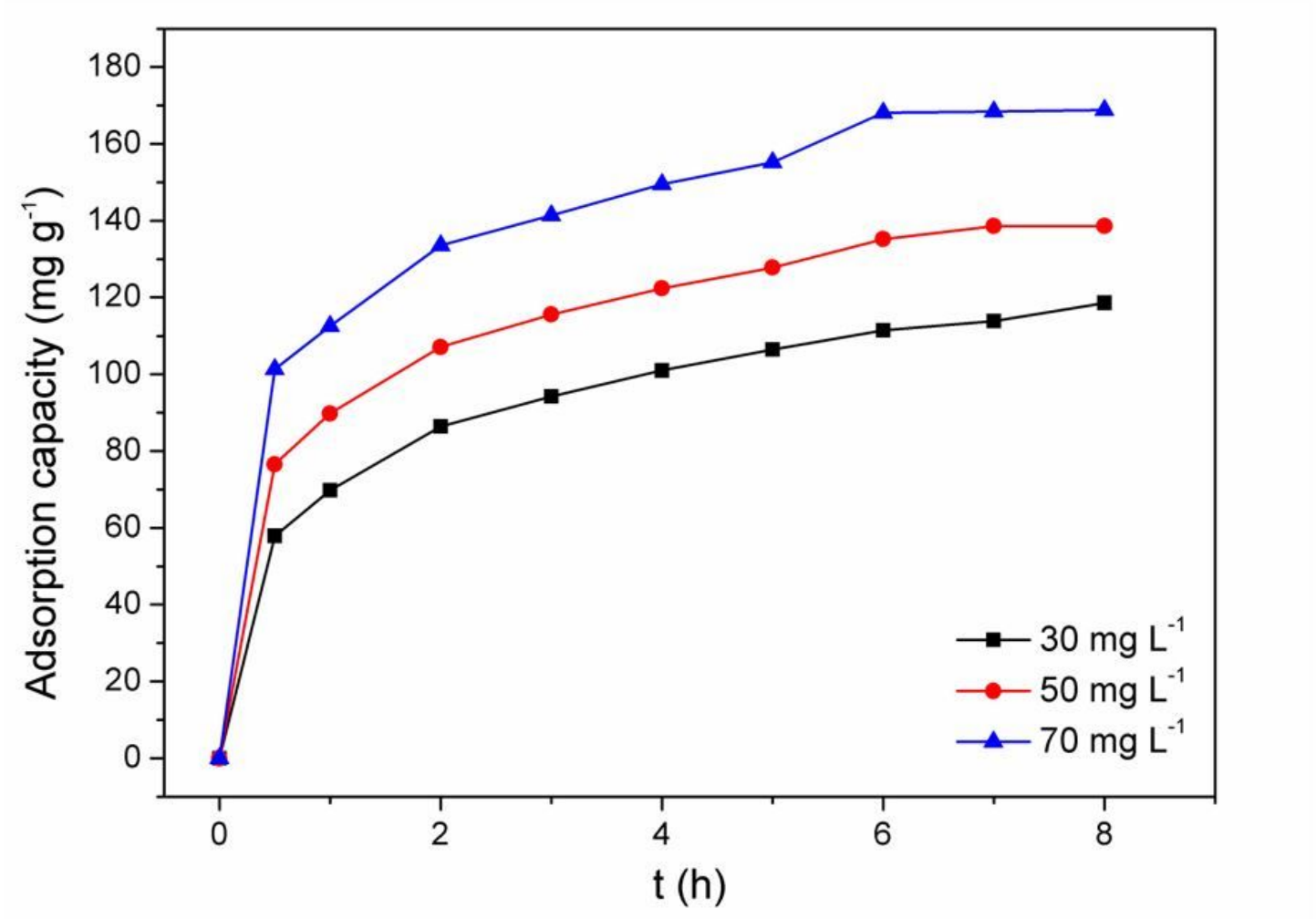

Figure 6

Effect of adsorption time on Cr(VI) adsorption by PEI/MoS2-10 at temperature of 25oC

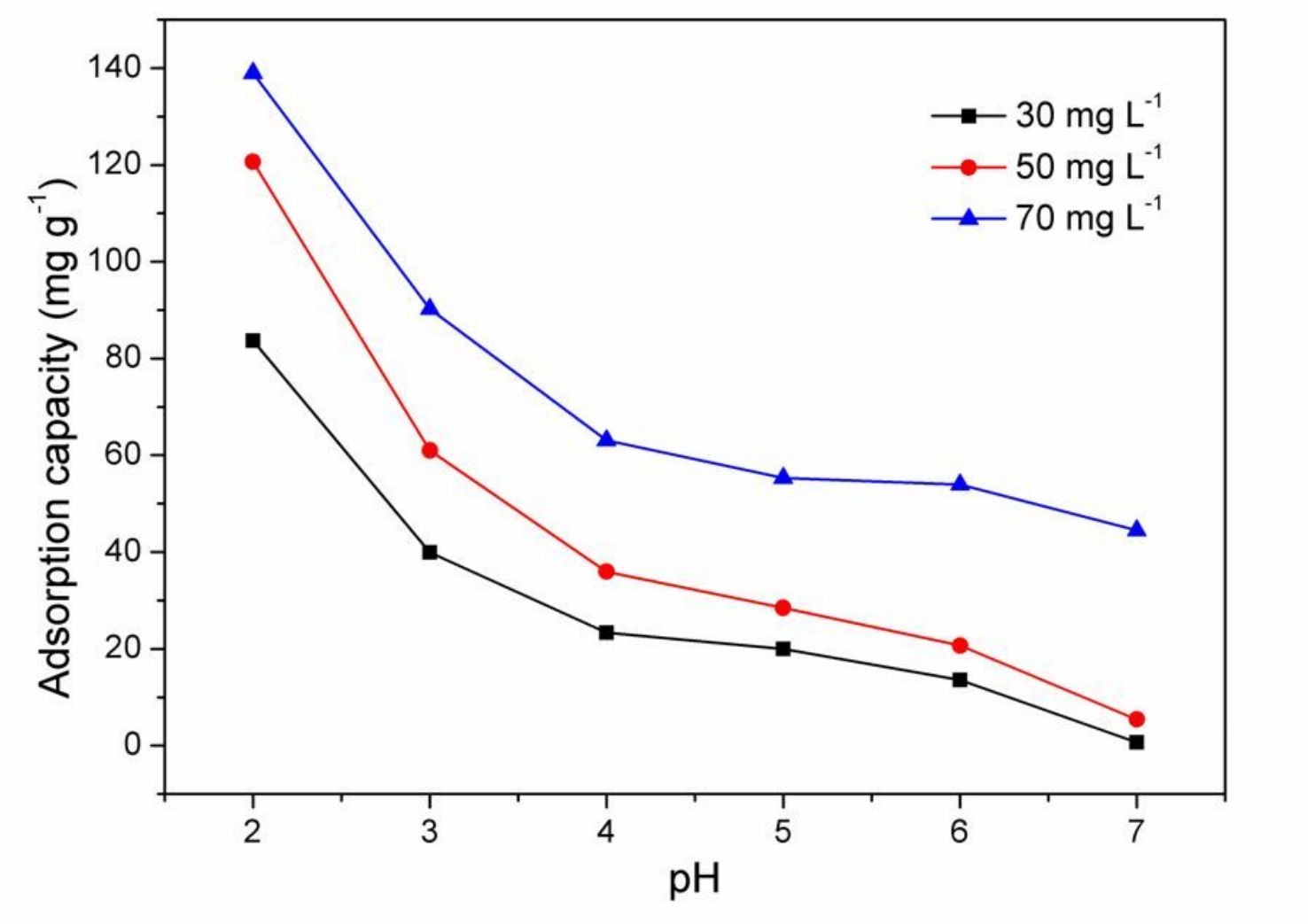

Figure 7

Effect of solution pH on Cr(VI) adsorption by PEI/MoS2-10, temperature of 25oC, adsorption time of 6 h

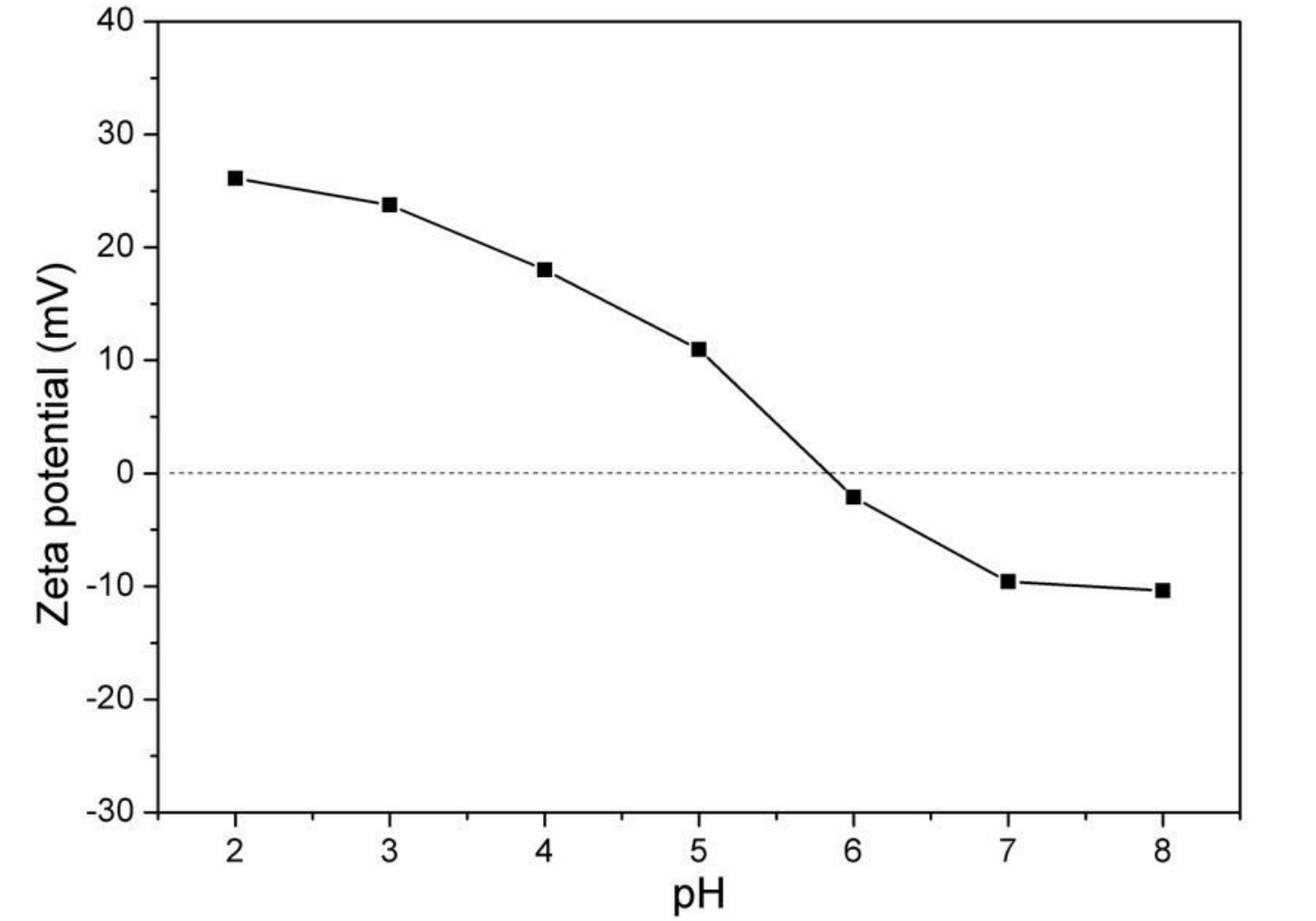

Figure 8

PZC of PEI/MoS2-10

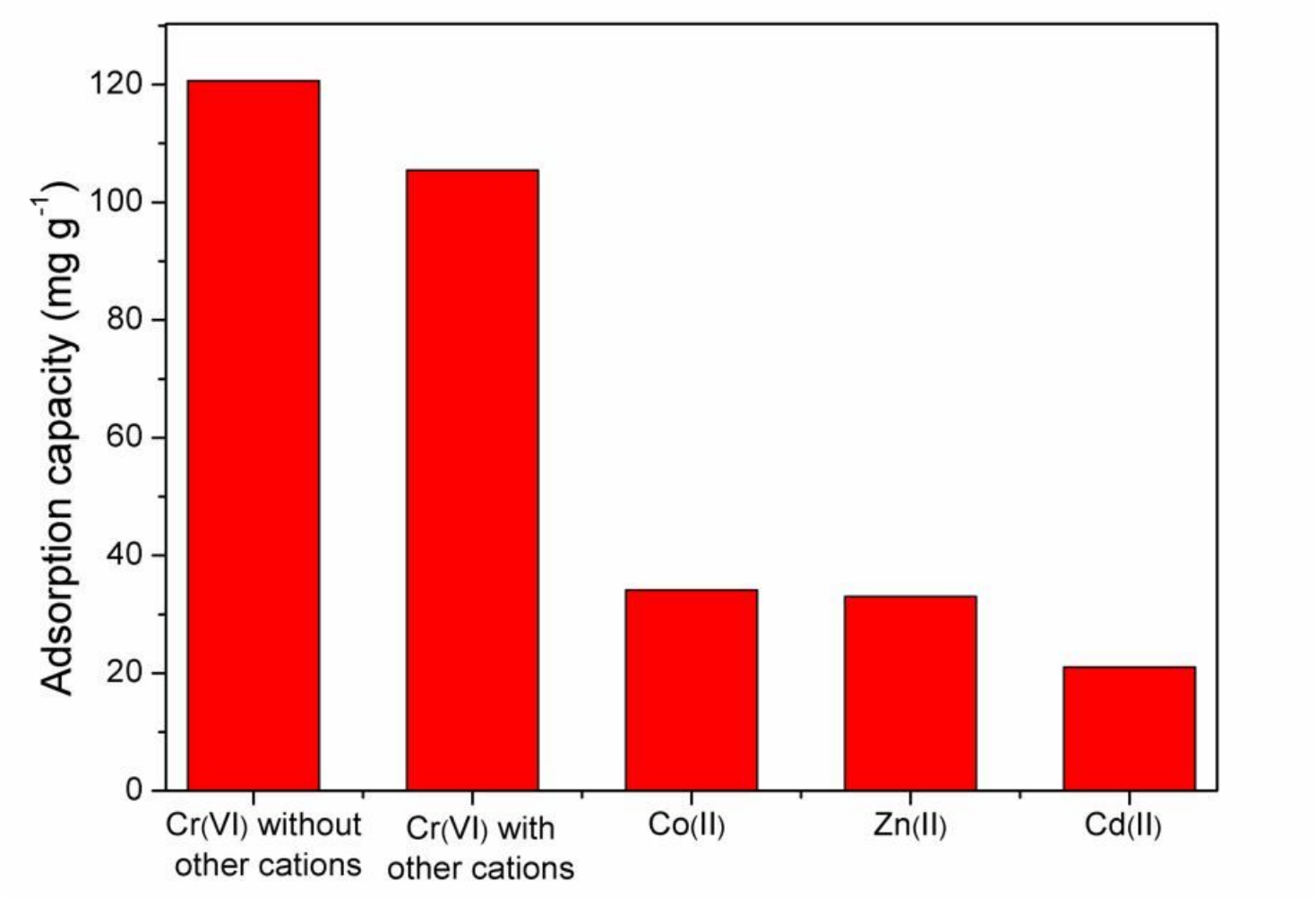

Figure 9

Effect of interference ion on Cr (VI) adsorption by PEI/MoS2-10, solution pH of 2, temperature of 25oC, adsorption time of 6 h

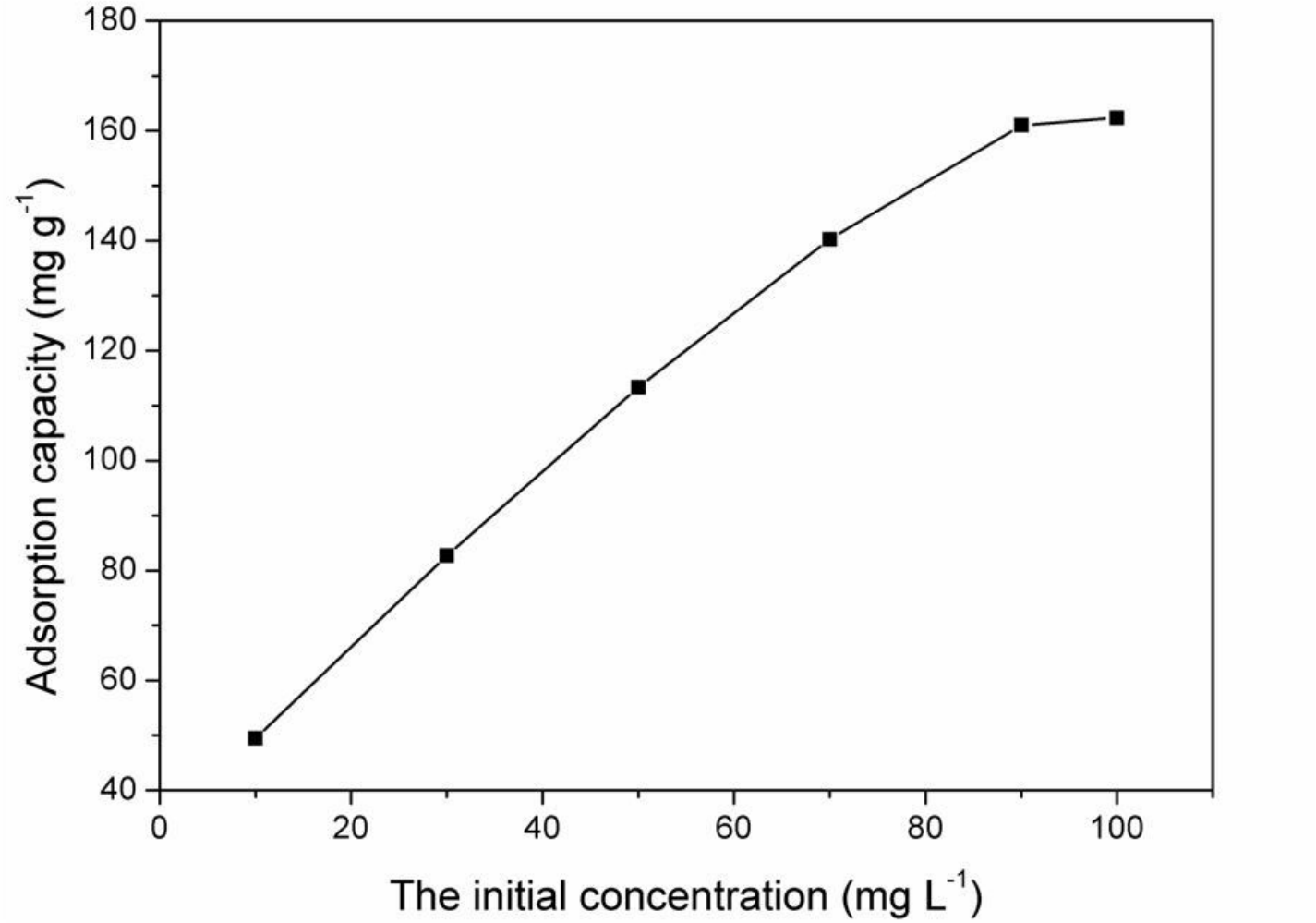

Figure 10

Effect of initial Cr(VI) concentration on adsorption by PEI/MoS2-10, solution pH of 2, temperature of 25oC, adsorption time of 6 h

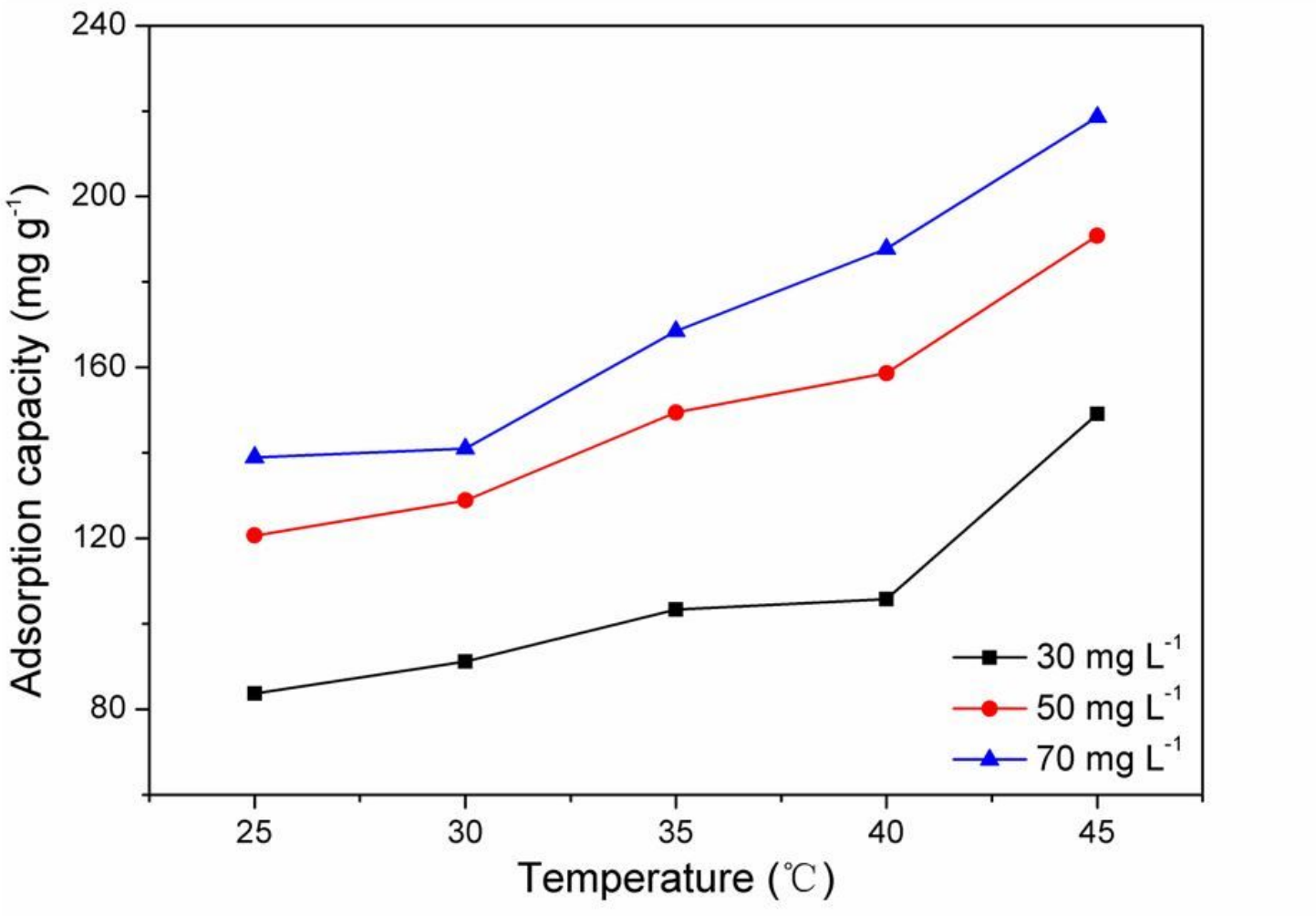

Figure 11

Effect of temperature on Cr(VI) adsorption, T = 6 h, initial Cr(VI) is 30, 50, 70 mg L-1

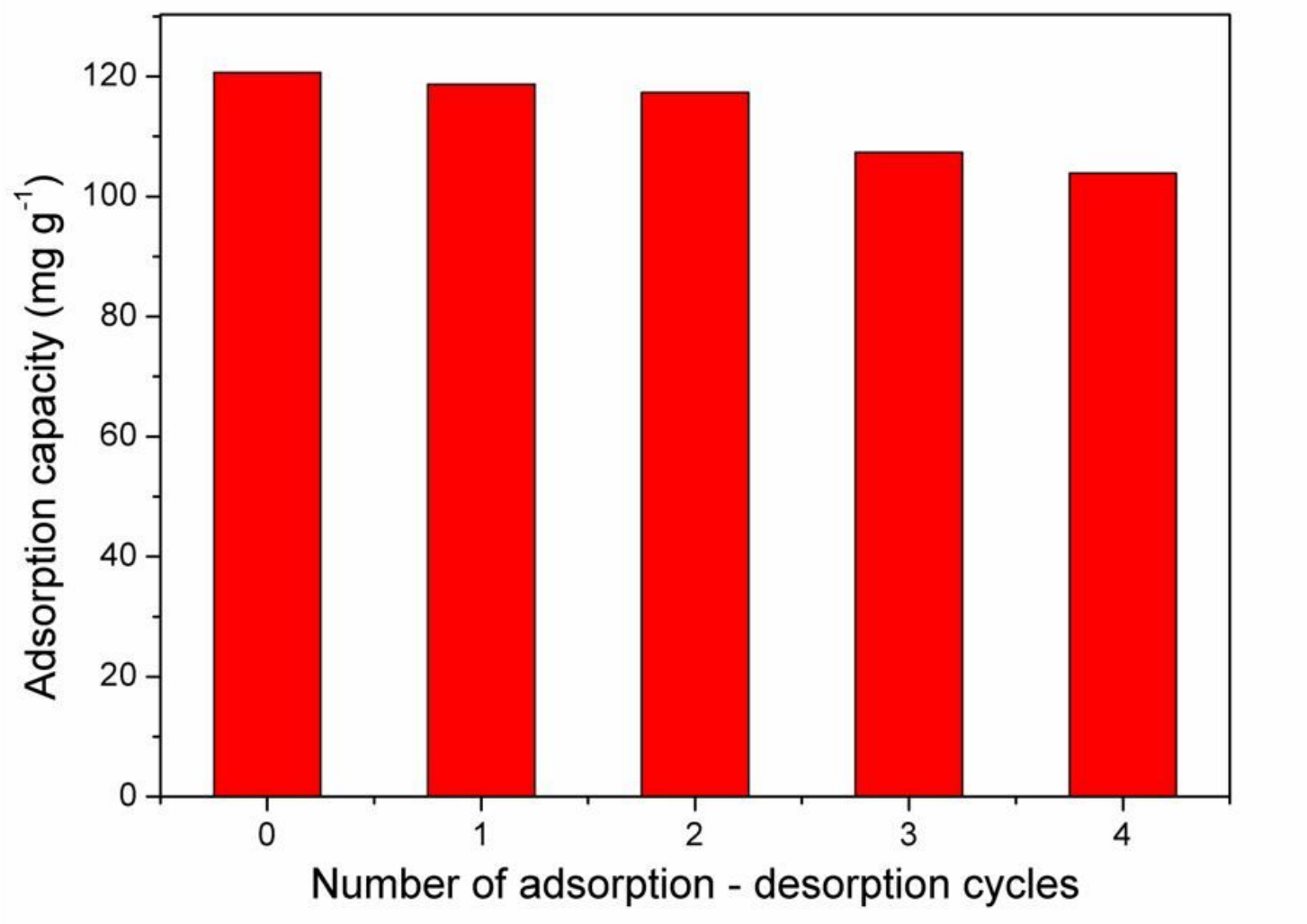

Figure 12

Cyclic tests of PEI/MoS2-10, T = 6 h, temperature of 25oC, initial Cr(VI) is 50 mg L-1

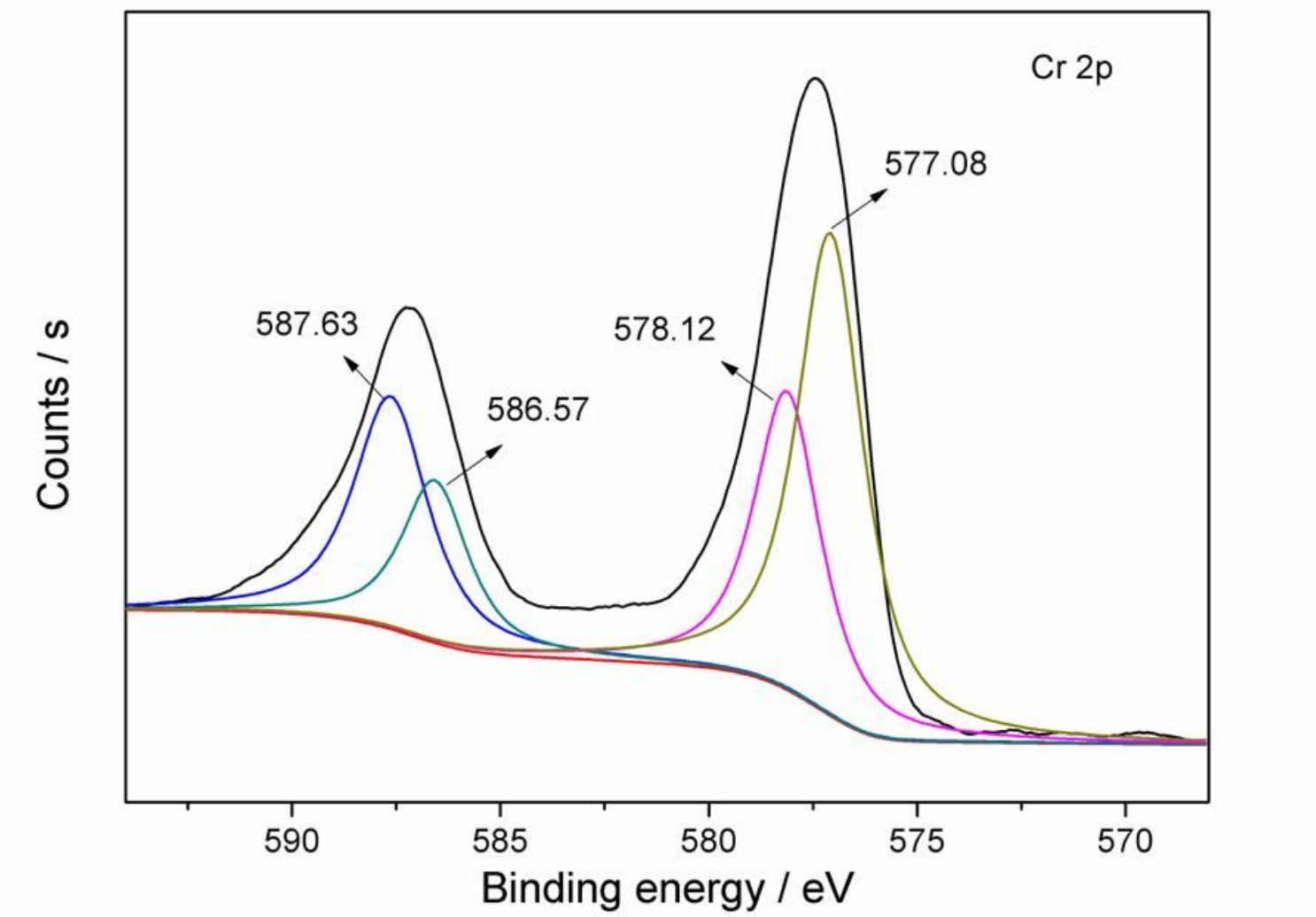

Figure 13

Binding spectrum of Cr 2p containing chromium